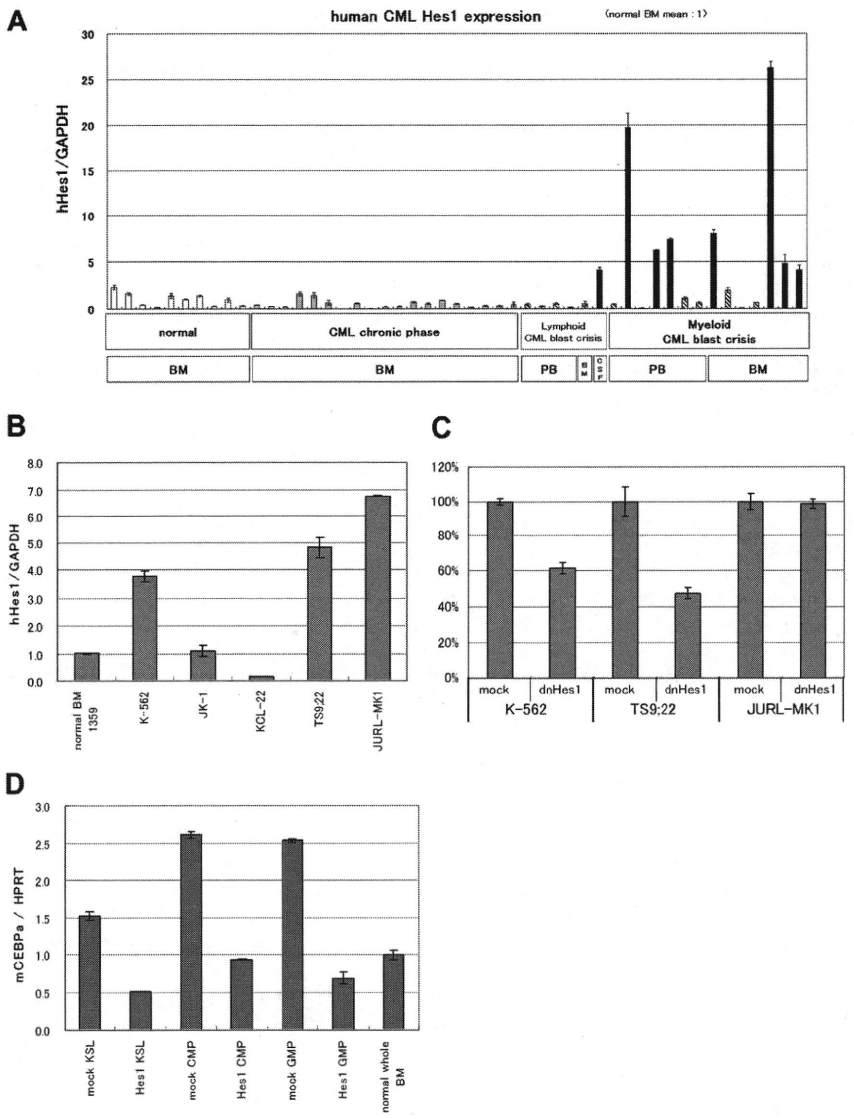

Figure 6. Hes1 expression was elevated in approximately 40% of patients with CML in blast crisis. (A) Real-time RT-PCR for Hes1 in bone marrow or peripheral blood cells from healthy subjects, patients with CML in chronic phase, or patients with CML in blast crisis. Expression levels were normalized by GAPDH mRNA. RNA from normal bone marrow cells served as a control (mean of 10 RNA levels of normal bone marrow was defined as 1). Hes1 mRNA levels exceeded 4 (solid bar) in 8 of 20 samples from CML in blast crisis patients. The correlation coefficient determined by the Wilcoxon signed-rank test between blast ratio and Hes1-expression level was −0.395. PB indicates peripheral blood; BM, bone marrow; CSF, cerebrospinal fluid. The solid bar represents CML in blast crisis exceeding 4; the hatched bar represents CML in blast crisis less than 4. (B) Hes1 expression in 5 human CML blast crisis cell lines. Expression levels of HES1 in K-562, JK-1, KCL-22, TS9:22, and JURL-MK1 were evaluated by real-time RT-PCR and were normalized by GAPDH mRNA. (C) Growth repression by transduction of dnHes1 (a dominant-negative Hes1) retrovirus vector into 3 human cell lines (K-562, TS9:22, and JURL-MK1). Six days after retrovirus transduction, cell numbers were counted. Growth is shown as a percentage of the control cells that were transduced with control vector. A representative result from 2 independent and reproducible experiments is shown. Error bars represent the SD from duplicate cultures. (D) Real-time RT-PCR for C/EBP-α in Hes1-transduced KSLs, CMPs, and GMPs compared with control vector-transduced KSLs, CMPs and GMPs. Total RNA was extracted at 60 hours from the initiation of Hes1-transduction. Error bars represent the SD from 2 independent experiments in (A-B,D).

in chronic phase patients. Although it is yet to be confirmed by a larger number of samples from CML as well as AML patients, this result indicates an interesting connection between the mouse model of AML/CML in blast crisis-like disease and human leukemia. In addition, we have demonstrated that transduction of dnHes1 represses the proliferation in 2 of 3 human cell lines of CML in blast crisis. These results suggest that Hes1 plays an important role in blast crisis of CML.

Although the origin of CML is considered to be a hematopoietic stem cell, blast crisis has been shown to be a result of transformation of myeloid progenitors.[16] BCR-ABL can cause MPN-like disease when introduced into the hematopoietic stem cell population but cannot induce MPN or leukemia when introduced into differentiated myeloid progenitors.[26] Therefore, development of full-blown AML/CML in blast crisis-like disease in mice with differentiated progenitors only by cotransduction with Hes1 and BCR-ABL may represent a true model of blast crisis of CML. In this context, Hes1 is a possible crisis-promoting gene like other examples, such as activated β-catenin[16] and BCL-2,[45] both of which caused CML in blast crisis-like disease in mice when transduced into GMPs together with BCR-ABL.

Several AML-associated fusion gene products, such as MLL-ENL,[46] MOZ-TIF2,[26] and MLL-AF9,[47] have been demonstrated to confer replating capacity on CMPs and GMPs, and eventually to transform these cells into leukemia-initiating cells. Unique to our findings is the fact that we transduced a wild-type transcription factor, Hes1, and found that such simple up-regulation of a transcription factor led to similar transformation phenotypes. A substantial number of examples have indicated that loss of function or altered function, rather than gain of function, of transcription factors, including MLL, MOZ, Runx1, RARα, C/EBP-α, etc, is associated with leukemogenesis. If up-regulation of Hes1 is indeed involved in human leukemias, this represents a new mechanism of leukemogenesis.

In modeling CML in mice, the present model provides a powerful tool by which we can induce 2 distinct phases of CML from stem cells or progenitors using BCR-ABL gene: a chronic phase-like state by transduction of KSL with BCR-ABL alone and a blast crisis-like state by cotransduction of CMPs and GMPs with BCR-ABL and Hes1.

In conclusion, we have developed a useful mouse model for CML blast crisis and have indicated that Hes1 is a key molecule in blast crisis transition in CML. The present mouse model will aid

Table 1. Clinical data of 20 patients with CML in blast crisis

Sample name	Source	Blast ratio	Hes1/GAPDH	Phenotype	Chromosome aberration	Clinical features
228 CML BC	PB	57	0.49	B-ALL	46,XY,t(9;22)/46,XY, +der(1;14)(q10;q12),t(9;22)	—
428 CML BC	PB	100	0.27	B-ALL	t(9;22)	—
984 CML BC	PB	60	0.56	B-ALL	46, XX, t(9;22)(q34;q11.2)	—
3259 CML BC	PB	100	0.16	B-ALL	t(9;22)	—
1385 CML BC	BM	81	0.56	B-ALL	t(9;22)	—
1107 CML BC	CSF	100	4.16	B-ALL	t(9;22)	The blasts increased drastically in CNS.
1 CML BC	PB	90	0.51	Myeloid	t(9;22)	—
219 CML BC	PB	12	19.72	Myeloid	45,XX,-7,t(9;22)	BM was dry tap composed of 100% blasts.
393 CML BC	PB	20	0.08	Myeloid	46,XX,t(9;22),add(17)(p11)	—
1088 CML BC	PB	30	6.22	Myeloid	46, XX, t(9;22)(q34;q11.2)	BM was dry tap.
1299 CML BC	PB	20	7.35	Myeloid	t(9;22)	BM was dry tap composed of 23% blasts.
1824 CML BC	PB	51	1.15	Myeloid	t(9;22)	BM was dry tap.
3153 CML BC	PB	7	0.66	Myeloid	t(9;22)	BM was dry tap. The blasts in BM increased up to 42% after taking this sample.
232 CML BC	BM	11	7.96	Myeloid	47,XY,+8,t(9;22)	The blasts in BM increased drastically up to 44% after taking this sample.
452 CML BC	BM	54	2.01	Myeloid	46,dic(17)(q10),t(9;22)	—
916 CML BC	BM	24	0.11	Myeloid	t(9;22)	—
1091 CML BC	BM	28	0.67	Myeloid	t(9;22)	—
811 CML BC	BM	25	26.25	Myeloid	46, XX, t(1;9;22)(q44;q34;q11.2)	—
3332 CML BC	BM	22	4.17	Myeloid	t(9;22)	—
3847 CML BC	BM	62	4.79	Myeloid	t(9;22)	—

CML indicates chronic myelogenous leukemia; BC, blast crisis; PB, peripheral blood; B-ALL, B-cell acute lymphoblastic leukemia; BM, bone marrow; CSF, cerebrospinal fluid; —, not applicable; and CNS, central nervous system.

understanding of the molecular mechanisms underlying blast crisis of CML and might lead to a better therapeutic outcome for this difficult disease.

Acknowledgments

The authors thank Dr R. Kageyama for the Hes1 cDNA; Dr H. Nakauchi and Dr M. Onodera for the GCDNsam/IRES-NGFR vector and the GCDNsam/IRES-GFP vector; Dr K. Akashi and Dr S. Mizuno for mouse C/EBP-α cDNA; Dr T. Inaba and Dr H. Asou (Hiroshima University, Hiroshima, Japan) for the JK-1, KCL-22, JURL-MK1 cell line; and Kirin Pharma for the TPO.

This work was supported by a Grant-in-Aid for Scientific Research (KAKENHI no. 20249051) and the Global Center of Excellence Program Center of Education and Research for the Advanced Genome-Based Medicine (for personalized medicine and the control of worldwide infectious diseases); the Ministry of Education, Culture, Sports, Science, and Technology of Japan (MEXT) and the Ministry of Health and Welfare of Japan (T.K.); and KAKENHI (no. 19390258), Astellas Foundation for Research on Metabolic Disorders, Uehara Memorial Foundation, and Princess Takamatsu Cancer Research Fund (S.C.).

Authorship

Contribution: F.N. did all the experiments and participated actively in writing the manuscript; M.S.-Y. and J.K. assisted with the experiments and actively participated in designing the experiments; Y.K., N.K., T.U., K.H., and K.K. assisted with the experiments; Y.H. and H.H. provided human samples; S.O. and M.K. participated in interpretation and designing the experiments; and T.K. and S.C. conceived the project, secured funding, and actively participated in manuscript writing.

Conflict-of-interest disclosure: T.K. serves as a consultant for R&D Systems and Rigel Pharmaceuticals. The remaining authors declare no competing financial interests.

Correspondence: Toshio Kitamura, Division of Stem Cell Signaling, Center for Stem Cell Therapy, Institute of Medical Science, University of Tokyo, 4-6-1 Shirokanedai, Minato-ku, Tokyo 108-8639, Japan; e-mail: kitamura@ims.u-tokyo.ac.jp; and Shigeru Chiba, Department of Hematology, Graduate School of Comprehensive Human Sciences, University of Tsukuba, 1-1-1 Tennodai, Tsukuba, Ibaraki 305-8575, Japan; e-mail: schiba-tky@umin.net.

References

1. Kageyama R, Nakanishi S. Helix-loop-helix factors in growth and differentiation of the vertebrate nervous system. *Curr Opin Genet Dev.* 1997;7(5):659-665.
2. Jarriault S, Brou C, Logeat F, Schroeter EH, Kopan R, Israel A. Signalling downstream of activated mammalian Notch. *Nature.* 1995;377(6547):355-358.
3. Jarriault S, Le Bail O, Hirsinger E, et al. Delta-1 activation of notch-1 signaling results in HES-1 transactivation. *Mol Cell Biol.* 1998;18(12):7423-7431.
4. Johnson JE, Birren SJ, Anderson DJ. Two rat homologues of Drosophila achaete-scute specifically expressed in neuronal precursors. *Nature.* 1990;346(6287):858-861.
5. Sumazaki R, Shiojiri N, Isoyama S, et al. Conversion of biliary system to pancreatic tissue in Hes1-deficient mice. *Nat Genet.* 2004;36(1):83-87.
6. Kumano K, Chiba S, Shimizu K, et al. Notch1 inhibits differentiation of hematopoietic cells by sustaining GATA-2 expression. *Blood.* 2001;98(12):3283-3289.
7. Kunisato A, Chiba S, Nakagami-Yamaguchi E, et al. HES-1 preserves purified hematopoietic stem cells ex vivo and accumulates side population cells in vivo. *Blood.* 2003;101(5):1777-1783.
8. Kaneta M, Osawa M, Sudo K, Nakauchi H, Farr AG, Takahama Y. A role for pref-1 and HES-1 in thymocyte development. *J Immunol.* 2000;164(1):256-264.
9. Tomita K, Hattori M, Nakamura E, Nakanishi S, Minato N, Kageyama R. The bHLH gene Hes1 is essential for expansion of early T cell precursors. *Genes Dev.* 1999;13(9):1203-1210.
10. Weng AP, Ferrando AA, Lee W, et al. Activating mutations of NOTCH1 in human T cell acute lymphoblastic leukemia. *Science.* 2004;306(5694):269-271.
11. Lee S-y, Kumano K, Nakazaki K, et al. Gain-of-function mutations and copy number increases of

Notch2 in diffuse large B-cell lymphoma. *Cancer Sci.* 2009;100(5):920-926.

12. Radtke F, Wilson A, Mancini SJ, MacDonald HR. Notch regulation of lymphocyte development and function. *Nat Immunol.* 2004;5(3):247-253.
13. Allman D, Punt JA, Izon DJ, Aster JC, Pear WS. An invitation to T and more: notch signaling in lymphopoiesis. *Cell.* 2002;109[suppl]:S1-S11.
14. Radtke F, Wilson A, Stark G, et al. Deficient T cell fate specification in mice with an induced inactivation of Notch1. *Immunity.* 1999;10(5):547-558.
15. Sakata-Yanagimoto M, Nakagami-Yamaguchi E, Saito T, et al. Coordinated regulation of transcription factors through Notch2 is an important mediator of mast cell fate. *Proc Natl Acad Sci U S A.* 2008;105(22):7839-7844.
16. Jamieson CH, Ailles LE, Dylla SJ, et al. Granulocyte-macrophage progenitors as candidate leukemic stem cells in blast-crisis CML. *N Engl J Med.* 2004; 351(7):657-667.
17. Akashi K, Traver D, Miyamoto T, Weissman IL. A clonogenic common myeloid progenitor that gives rise to all myeloid lineages. *Nature.* 2000; 404(6774):193-197.
18. Honda H, Fujii T, Takatoku M, et al. Expression of p210bcr/abl by metallothionein promoter induced T-cell leukemia in transgenic mice. *Blood.* 1995; 85(10):2853-2861.
19. Kitamura T, Koshino Y, Shibata F, et al. Retrovirus-mediated gene transfer and expression cloning: powerful tools in functional genomics. *Exp Hematol.* 2003;31(11):1007-1014.
20. Morita S, Kojima T, Kitamura T. Plat-E: an efficient and stable system for transient packaging of retroviruses. *Gene Ther.* 2000;7(12):1063-1066.
21. Sang L, Coller HA, Roberts JM. Control of the reversibility of cellular quiescence by the transcriptional repressor HES1. *Science.* 2008; 321(5892):1095-1100.
22. Hopfer O, Zwahlen D, Fey MF, Aebi S. The Notch pathway in ovarian carcinomas and adenomas. *Br J Cancer.* 2005;93(6):709-718.
23. Iwasaki H, Mizuno S, Mayfield R, et al. Identification of eosinophil lineage-committed progenitors in the murine bone marrow. *J Exp Med.* 2005; 201(12):1891-1897.
24. Ono R, Nakajima H, Ozaki K, et al. Dimerization of MLL fusion proteins and FLT3 activation synergize to induce multiple-lineage leukemogenesis. *J Clin Invest.* 2005;115(4):919-929.
25. Kawamata S, Du C, Li K, Lavau C. Overexpression of the Notch target genes Hes in vivo induces lymphoid and myeloid alterations. *Oncogene.* 2002;21(24):3855-3863.
26. Huntly BJ, Shigematsu H, Deguchi K, et al. MOZ-TIF2, but not BCR-ABL, confers properties of leukemic stem cells to committed murine hematopoietic progenitors. *Cancer Cell.* 2004;6(6):587-596.
27. Lozzio CB, Lozzio BB. Human chronic myelogenous leukemia cell-line with positive Philadelphia chromosome. *Blood.* 1975;45(3):321-334.
28. Okuno Y, Suzuki A, Ichiba S, et al. Establishment of an erythroid cell line (JK-1) that spontaneously differentiates to red cells. *Cancer.* 1990;66(7): 1544-1551.
29. Kubonishi I, Miyoshi I. Establishment of a Ph1 chromosome-positive cell line from chronic myelogenous leukemia in blast crisis. *Int J Cell Cloning.* 1983;1(2):105-117.
30. Gotoh A, Miyazawa K, Ohyashiki K, et al. Tyrosine phosphorylation and activation of focal adhesion kinase (p125FAK) by BCR-ABL oncoprotein. *Exp Hematol.* 1995;23(11):1153-1159.
31. Di Noto R, Luciano L, Lo Pardo C, et al. JURL-MK1 (c-kit(high)/CD30-/CD40-) and JURL-MK2 (c-kit(low)/CD30+/CD40+) cell lines: 'two-sided' model for investigating leukemic megakaryocytopoiesis. *Leukemia.* 1997;11(9):1554-1564.
32. Lee SY, Kumano K, Masuda S, et al. Mutations of the Notch1 gene in T-cell acute lymphoblastic leukemia: analysis in adults and children. *Leukemia.* 2005;19(10):1841-1843.
33. Allenspach EJ, Maillard I, Aster JC, Pear WS. Notch signaling in cancer. *Cancer Biol Ther.* 2002;1(5):466-476.
34. Fu L, Kogoshi H, Nara N, Tohda S. NOTCH1 mutations are rare in acute myeloid leukemia. *Leuk Lymphoma.* 2006;47(11):2400-2403.
35. Ingram WJ, McCue KI, Tran TH, Hallahan AR, Wainwright BJ. Sonic Hedgehog regulates Hes1 through a novel mechanism that is independent of canonical Notch pathway signalling. *Oncogene.* 2008;27(10):1489-1500.
36. Kamakura S, Oishi K, Yoshimatsu T, Nakafuku M, Masuyama N, Gotoh Y. Hes binding to STAT3 mediates crosstalk between Notch and JAK-STAT signalling. *Nat Cell Biol.* 2004;6(6):547-554.
37. Nerlov C. C/EBPalpha mutations in acute myeloid leukaemias. *Nat Rev Cancer.* 2004;4(5):394-400.
38. Gombart AF, Hofmann WK, Kawano S, et al. Mutations in the gene encoding the transcription factor CCAAT/enhancer binding protein alpha in myelodysplastic syndromes and acute myeloid leukemias. *Blood.* 2002;99(4):1332-1340.
39. Smith ML, Cavenagh JD, Lister TA, Fitzgibbon J. Mutation of CEBPA in familial acute myeloid leukemia. *N Engl J Med.* 2004;351(23):2403-2407.
40. Zhang P, Iwasaki-Arai J, Iwasaki H, et al. Enhancement of hematopoietic stem cell repopulating capacity and self-renewal in the absence of the transcription factor C/EBP alpha. *Immunity.* 2004;21(6):853-863.
41. Koschmieder S, Halmos B, Levantini E, Tenen DG. Dysregulation of the C/EBPalpha differentiation pathway in human cancer. *J Clin Oncol.* 2009;27(4):619-628.
42. Kirstetter P, Schuster MB, Bereshchenko O, et al. Modeling of C/EBPalpha mutant acute myeloid leukemia reveals a common expression signature of committed myeloid leukemia-initiating cells. *Cancer Cell.* 2008;13(4):299-310.
43. Fan X, Mikolaenko I, Elhassan I, et al. Notch1 and notch2 have opposite effects on embryonal brain tumor growth. *Cancer Res.* 2004;64(21): 7787-7793.
44. Hallahan AR, Pritchard JI, Hansen S, et al. The SmoA1 mouse model reveals that notch signaling is critical for the growth and survival of sonic hedgehog-induced medulloblastomas. *Cancer Res.* 2004;64(21):7794-7800.
45. Jaiswal S, Traver D, Miyamoto T, Akashi K, Lagasse E, Weissman IL. Expression of BCR/ABL and BCL-2 in myeloid progenitors leads to myeloid leukemias. *Proc Natl Acad Sci U S A.* 2003;100(17):10002-10007.
46. Cozzio A, Passegue E, Ayton PM, Karsunky H, Cleary ML, Weissman IL. Similar MLL-associated leukemias arising from self-renewing stem cells and short-lived myeloid progenitors. *Genes Dev.* 2003;17(24):3029-3035.
47. Krivtsov AV, Twomey D, Feng Z, et al. Transformation from committed progenitor to leukaemia stem cell initiated by MLL-AF9. *Nature.* 2006;442(7104): 818-822.

Derivation of functional mature neutrophils from human embryonic stem cells

Yasuhisa Yokoyama,[1-3] Takahiro Suzuki,[1,2,4] Mamiko Sakata-Yanagimoto,[1-3] Keiki Kumano,[1,2] Katsumi Higashi,[5] Tsuyoshi Takato,[4] Mineo Kurokawa,[2] Seishi Ogawa,[1,4,6] and Shigeru Chiba[1,3]

[1]Department of Cell Therapy and Transplantation Medicine, University of Tokyo Hospital, Tokyo; [2]Department of Hematology and Oncology, Graduate School of Medicine, University of Tokyo, Tokyo; [3]Department of Clinical and Experimental Hematology, University of Tsukuba, Ibaraki; [4]Divison of Tissue Engineering, University of Tokyo Hospital, Tokyo; [5]Department of Clinical Hematology, School of Health Sciences, Kyorin University, Tokyo; and [6]The 21st Century COE Program, Graduate School of Medicine, University of Tokyo, Tokyo, Japan

Human embryonic stem cells (hESCs) proliferate infinitely and are pluripotent. Only a few reports, however, describe specific and efficient methods to induce hESCs to differentiate into mature blood cells. It is important to determine whether and how these cells, once generated, behave similarly with their in vivo–produced counterparts. We developed a method to induce hESCs to differentiate into mature neutrophils. Embryoid bodies were formed with bone morphogenic protein-4, stem cell factor (SCF), Flt-3 ligand (FL), interleukin-6 (IL-6)/IL-6 receptor fusion protein (FP6), and thrombopoietin (TPO). Cells derived from the embryoid bodies were cultured on a layer of irradiated OP9 cells with a combination of SCF, FL, FP6, IL-3, and TPO, which was later changed to granulocyte–colony-stimulating factor. Morphologically mature neutrophils were obtained in approximately 2 weeks with a purity and efficiency sufficient for functional analyses. The population of predominantly mature neutrophils (hESC-Neu's) showed superoxide production, phagocytosis, bactericidal activity, and chemotaxis similar to peripheral blood neutrophils from healthy subjects, although there were differences in the surface antigen expression patterns, such as decreased CD16 expression and aberrant CD64 and CD14 expression in hESC-Neu's. Thus, this is the first description of a detailed functional analysis of mature hESC-derived neutrophils. (Blood. 2009;113:6584-6592)

Introduction

Embryonic stem (ES) cells can self-renew and differentiate into cells derived from all 3 germ layers (ie, ectoderm, endoderm, and mesoderm). Both mouse and human ES cells give rise to mature blood cells of granulocyte/macrophage, erythroid, and megakaryoid lineages in vitro. For blood cell induction from ES cells, the majority of investigators use a coculturing system with mouse stromal cells such as S17[1] or OP9.[2,3] Embryoid body (EB) formation is also a commonly used method to obtain starting materials for further culture.[4-6] Cell surface antigens, such as CD45 and CD34, and colony-forming ability are used as blood cell markers. Hemangioblasts, which have the capacity to differentiate into both endothelial and blood cells, have also been produced.[7-9] Only a few studies, however, have achieved specific and effective induction of mature blood cells from ES cells, particularly human ES cells (hESCs).[10]

Human ESC-derived blood cells are potentially useful as a replacement for donation-based blood for transfusion in clinical settings, for drug discovery screening, and for monitoring drug efficacy and toxicity. The current blood donation system for transfusion is incapable of providing enough granulocytes for patients with life-threatening neutropenia, although granulocyte transfusion could have a potentially significant benefit for a certain population of severely neutropenic patients.[11,12] Given the large amount of neutrophils required for transfusion,[13] hESC-derived neutrophils might be a unique solution for this treatment demand. Therefore, the development of a highly effective method of neutrophil differentiation from hESCs is an important step for both clinical application of hESCs and granulocyte transfusion medicine.

The lack of an effective method for obtaining hESC-derived neutrophils with purity sufficient for functional analysis, however, has hampered progress in this field. Once neutrophils with a high purity can be generated from hESCs, it will be important to compare their activities with those of neutrophils produced in vivo, particularly given the fact that hESCs rarely give rise to hematopoietic stem cells in vitro,[14] and thus, that hESC-derived neutrophils might not be a progeny of hematopoietic stem cells. Here, we developed an effective method of deriving mature neutrophils from hESCs through EB formation and subsequent coculture with OP9, and analyzed their morphologic and phenotypic characteristics. We then performed functional analyses of hESC-derived neutrophils in vitro, focusing on superoxide production, phagocytosis, bactericidal activity, and chemotaxis, in comparison with peripheral blood neutrophils (PB-Neu's) obtained from healthy subjects.

Methods

Human ES cell culture and EB formation

In all experiments using hESCs, we used KhES-3[15] cells (a kind gift from Dr Nakatsuji; Kyoto University, Kyoto, Japan), which were maintained as previously described.[16] Briefly, KhES-3 colonies were cultured on irradiated mouse embryonic fibroblasts in Dulbecco modified Eagle medium/F12 (Invitrogen, Carlsbad, CA) supplemented with 20% KNOCKOUT serum

Submitted May 31, 2008; accepted March 5, 2009. Prepublished online as *Blood* First Edition paper, March 25, 2009; DOI 10.1182/blood-2008-06-160838.

An Inside *Blood* analysis of this article appears at the front of this issue.

The publication costs of this article were defrayed in part by page charge payment. Therefore, and solely to indicate this fact, this article is hereby marked "advertisement" in accordance with 18 USC section 1734.

replacer (Invitrogen) and 2.5 ng/mL human basic fibroblast growth factor (Invitrogen). The culture medium was replaced daily with fresh medium. Colonies were passaged onto new mouse embryonic fibroblasts every 6 days. To induce the formation of EBs, KhES-3 colonies were picked up using collagenase, and cultured in suspension in nonserum stem cell medium that we previously used in a hematopoietic stem cell expansion protocol.[17] After 24 hours, the colonies formed EBs, which were collected and cultured further for 17 days in Iscove modified Dulbecco medium (IMDM; Invitrogen) containing 15% fetal bovine serum (FBS), 1% nonessential amino acid (Invitrogen), 2 mM L-glutamine, 100 U/mL penicillin, 100 μg/mL streptomycin, and 0.1 mM 2-mercaptoethanol (ME) supplemented with cytokines (25 ng/mL bone morphogenic protein-4 [R&D Systems, Minneapolis, MN], 50 ng/mL stem cell factor [SCF; R&D Systems], 50 ng/mL Flt-3 ligand [R&D Systems], 50 ng/mL interleukin-6 [IL-6]/IL-6 receptor fusion protein [FP6; Kyowa Hakko Kirin, Tokyo, Japan], and 20 ng/mL thrombopoietin [TPO; Kyowa Hakko Kirin]).

Expansion of hematopoietic progenitor cells and terminal differentiation into mature neutrophils on OP9 stromal cells

OP9 cells (a kind gift from Dr Nakano; Osaka University, Osaka, Japan) were irradiated with 20 Gy and plated onto gelatin-coated 6-well tissue culture plates at a density of 1.5×10^5/well. The next day, the EBs (incubated for 18 days after the initiation of suspension culture) were trypsinized and disrupted into single cells. Cells were suspended in the progenitor expansion medium (IMDM supplemented with 10% FBS, 10% horse serum [StemCell Technologies, Vancouver, BC], 5% protein-free hybridoma medium [Invitrogen], 0.1 mM 2-ME, 100 U/mL penicillin, 100 μg/mL streptomycin, 100 ng/mL SCF, Flt-3 ligand, FP6, and 10 ng/mL TPO and IL-3 [R&D Systems]) and plated onto the irradiated OP9 cells (day 0). Each well contained up to 5×10^5 EB-derived cells. The culture medium was replaced with fresh medium on day 4.

On day 7 of the progenitor expansion phase, floating cells were collected, suspended with terminal differentiation medium (IMDM supplemented with 10% FBS, 0.1 mM 2-ME, 100 U/mL penicillin, 100 μg/mL streptomycin, and 50 ng/mL granulocyte colony-stimulating factor [G-CSF; Kyowa Hakko Kirin]), and transferred onto the newly irradiated OP9 cells. The culture medium was replaced with fresh medium on day 10. This terminal differentiation phase culture was continued for 6 or 7 days.

Preparation of normal PB-Neu's and bone marrow mononuclear cells

Human peripheral blood and bone marrow cells were obtained from healthy adult donors after obtaining informed consent in accordance with the Declaration of Helsinki. The institutional review board of the University of Tsukuba approved the use of peripheral blood neutrophils in this research. PB-Neu's were prepared as previously described.[18] The purity of the neutrophils was greater than 90%, with the remaining cells mainly eosinophils. Neutrophils were suspended in Hanks balanced salt solution (HBSS; Invitrogen) containing 0.5% bovine serum albumin (BSA) and placed at 4°C. In some experiments, peripheral blood mononuclear cells (PB-MNCs) were collected from the intermediate layer after centrifugation with Lymphoprep (Axis-shield, Oslo, Norway). Bone marrow cells were directly centrifuged with Lymphoprep, and only mononuclear cells were collected. Bone marrow mononuclear cells (BM-MNCs) were used immediately for RNA extraction.

Wright-Giemsa, myeloperoxidase, and alkaline-phosphatase staining

The morphology and granule characteristics of hESC-derived cells at the indicated days were assessed by Wright-Giemsa staining, comparing them with normal PB-Neu's. Myeloperoxidase and alkaline-phosphatase staining was performed using the New PO-K staining kit and alkaline phosphatase staining kit (MUTO PURE CHEMICALS, Tokyo, Japan). The prepared slides were inspected using an Olympus BX51 microscope equipped with a 100 × /1.30 UPlan objective lens (Olympus, Tokyo, Japan). Images were acquired with an HC-2500 digital camera and Photograb-2500 software (Fujifilm, Tokyo, Japan).

Electron microscopy

After 13 or 14 days culture, the population contained predominantly morphologically mature neutrophils, and was defined as hESC-Neu's. The hESC-Neu's and PB-Neu's were fixed in 2% paraformaldehyde/2.5% glutaraldehyde in 0.1 M phosphate buffered saline (PBS; Invitrogen) for at least 12 hours, and then postfixed in 1% osmium tetroxide in 0.1 M PBS for 2 hours. After fixation, samples were dehydrated in a graded ethanol series, cleared with propylene oxide, and embedded in Epon. Thin sections of cured samples were stained with uranyl acetate and Reynolds lead citrate. The sections were inspected using a transmission electron microscope, H7000 (Hitachi, Tokyo, Japan).

Semiquantitative RT-PCR for lactoferrin

Total RNA was obtained from hESC-derived cells of indicated culture days, PB-Neu's, PB-MNC's, and BM-MNC's using an RNeasy mini kit (QIAGEN, Hilden, Germany), and cDNA was synthesized from each RNA sample using a random primer and SuperScript III (Invitrogen) following the manufacturer's protocol. Semiquantitative polymerase chain reaction (PCR) was performed as previously described.[19] The sequence information of gene-specific primers used in reverse transcription (RT)–PCR and the PCR conditions is available upon request.

Flow cytometric analysis

Surface antigens of hESC-derived cells harvested on the indicated days were analyzed by flow cytometry using fluorescence-activated cell sorting (FACS) Aria (Becton Dickinson Immunocytometry Systems, San Jose, CA). Fc receptors on the cells were blocked with PBS containing 2% FBS and FcR Blocking Reagent (Miltenyi Biotec, Bergisch Gladbach, Germany). Antigens were stained with either fluorescein isothiocyanate (FITC)–conjugated antihuman CD13, CD64, CD11b (Beckman Coulter, Fullerton, CA), or CD14 (BD Pharmingen, San Diego, CA) antibodies; phycoerythrin-conjugated antihuman CD16, CD32, CD33 (Beckman Coulter), CD11b, or CD45 (BD Pharmingen) antibodies; or allophycocyanin-conjugated antihuman CD15, CD117 (BD Pharmingen), CD34, or CD133 (Myltenyi Biotec) antibodies. The negative range was determined by referencing the fluorescence of isotype controls. Dead cells were detected using 7-amino-actinomycin D (Via-Probe; BD Pharmingen).

Apoptosis assay

Neutrophils (hESC-Neu's and PB-Neu's) were suspended in IMDM with 0.5% BSA and incubated in 6-well plates at 37°C with 5% CO_2, with or without 50 ng/mL G-CSF. At the indicated time, neutrophils were harvested, stained with FITC-conjugated Annexin V and propidium iodide (PI) using an Annexin V-FITC Kit (Beckman Coulter), and analyzed by FACS Aria. Cells negative for both Annexin V and PI were judged as live cells.

G-CSF stimulation prior to assessing neutrophil function

Because the functions of hESC-Neu's are modified by G-CSF in the culture medium, we stimulated hESC-Neu's and PB-Neu's (PB-Neu(G+)'s) for 15 minutes at 37°C with 50 ng/mL G-CSF in the reaction medium. As a control, PB-Neu's without G-CSF stimulation (PB-Neu(G−)'s) were prepared. hESC-Neu's, PB-Neu(G+)'s, and PB-Neu(G−)'s were used for functional assays directly without changing the medium.

Detection of reactive oxygen species produced by neutrophils

Neutrophil production of reactive oxygen species was detected by flow cytometry using dihydrorhodamine123 (DHR; Sigma-Aldrich, St Louis, MO) as described previously.[20-22] Briefly, 1×10^5 hESC-Neu's, PB-Neu(G+)'s, or PB-Neu(G−)'s were suspended in 400 μL of the reaction medium (HBSS containing 0.5% BSA) per tube, and 3 tubes were prepared of each sample. Catalase (Sigma-Aldrich) at a final concentration of 1000 U/mL, 1.8 μL 29 mM DHR, and 100 μL 3.2 μM phorbol myristate

acetate (PMA; Sigma-Aldrich) were added to 1 of the 3 tubes; either no DHR or only DHR was added in the other 2 tubes as controls. Reaction medium was added to bring the final volume up to 500 μL. After 15-minute reaction at 37°C, the samples were washed twice with ice-cold reaction medium, and suspended in 200 μL reaction medium. Rhodamine fluorescence from the oxidized DHR was detected using FACS Aria.

Phagocytosis and NBT-reduction test using NBT-coated yeast cells

Phagocytosis and NBT reduction were visualized in a single set of experiments. Autoclaved Baker yeast was suspended in 0.5% NBT solution (0.5% NBT [Sigma-Aldrich] and 0.85% sodium chloride in distilled water) at a density of 1×10^8/mL. A 5-μL aliquot of this yeast suspension was added to hESC-Neu's, PB-Neu(G+)'s, and PB-Neu(G−)'s at 2.5×10^5 in 50 μL FBS. After 1 hour at 37°C, the samples were washed and stained with 1% safranin-O (MUTO PURE CHEMCALS) for 5 minutes. The samples were then washed twice and suspended in 100 μL PBS. A small aliquot of each sample was placed onto a glass slide and topped with a cover glass, and the number of ingested yeast cells and their change in color from brown to purple or black were examined using a microscope. Ingested yeast cells that changed color in the cells were counted as NBT-reaction positive, whereas those that were ingested but did not change color were counted as NBT-reaction negative. The phagocytosis rate was calculated as the percentage of neutrophils that contained one or more NBT-positive yeast cells. The phagocytosis score was calculated as the total number of positive yeast cells in 100 neutrophils. Only morphologically determined neutrophils were scored, excluding contaminating cells such as macrophages, the percentage of which was less than 15% of the total cells.

Bacterial killing assay

The bacterial killing assay was performed using *Escherichia coli* ATCC25922 as previously described[23] with some modifications. Briefly, 1×10^8 colony-forming units (CFUs) of exponentially growing bacteria were suspended in 1 mL HEPES-buffered saline with 10% human AB serum (MP Biomedicals, Irvine, CA) and opsonized at 37°C for 30 minutes. Neutrophils (hESC-Neu's, PB-Neu(G−)'s, and PB-Neu(G+)'s) were suspended in HEPES-buffered saline with 40% human AB serum at a concentration of 5×10^6/mL. The opsonized *E coli* was added to the suspension of hESC-Neu's and PB-Neu's, at a neutrophil/bacteria ratio of 2:1, or control medium. After 1-hour incubation, 50 μL of samples with and without neutrophils were diluted in 2.5 mL alkalinized water (pH 11) for lysis of neutrophils. Samples were further diluted with PBS, and duplicate aliquots were added to molten tryptic soy broth with 1.5% agar kept at 42°C, rapidly mixed, and plated on dishes. The CFUs were counted after overnight incubation.

Chemotaxis assay

Chemotactic ability was determined using a modified Boyden chamber method.[24] Briefly, 700 μL of the reaction medium (HBSS containing 0.5% BSA) with or without 10^{-7} M formyl-Met-Leu-Phe (fMLP; Sigma-Aldrich) was placed into each well of a 24-well plate, and the cell culture insert (3.0-μm pores; Falcon; Becton Dickinson, Franklin Lakes, NJ) was gently placed into each well to divide the well into upper and lower sections. Neutrophils were suspended in the reaction medium at 2.5×10^6/mL and 200 μL cell suspension was added to the upper well, allowing the neutrophils to migrate from the upper to the lower side of the membrane for 90 minutes at 37°C. After incubation, the membranes were washed, fixed with methanol, stained with Carrazi hematoxylin (MUTO PURE CHEMICALS), and mounted on the slide glass. The number of neutrophils that migrated through the membrane from the upper to the lower side was counted using a microscope with a high-power lens (× 400) in 3 fields: 2 near the edge and 1 on the center. Only mature neutrophils were counted.

Statistical analyses

Results are expressed as mean plus or minus SD. Statistical significance was determined using a 2-tailed Student *t* test. Results were considered significant when *P* values were less than .05.

Results

Effective derivation of mature neutrophils from hESCs with high purity

After initiating the suspension culture of EB-derived cells, small clusters of round-shaped cells appeared on the OP9 stromal layer around day 4. The morphology of the day-7 cells visualized with Wright-Giemsa staining suggested that they were myeloblasts and promyelocytes. On days 9 and 11, myelocytes and metamyelocytes were predominant, and on day 13 or 14, 70% to 80% of the cells appeared to be stab and segmented neutrophils (Figure 1A), with approximately 90% of the granulocytes at the metamyelocyte stage or later (Table 1). This finding indicated that hESC-derived cells differentiated into mature neutrophils by a process similar to physiologic granulopoiesis. The remaining cells appeared to be macrophages or monocytes, and cells of other lineages, such as erythroid or lymphoid cells, were not observed at any time during the culture. The number of total cells peaked around days 9 to 11, with an average 2.9-fold increase (range; 0.5- to 10.0-fold in 23 independent cultures) compared with the initial EB-derived cell number. The final yield of the cells on day 13 or 14 was 1.7-fold (range; 0.1- to 8.8-fold in 28 independent cultures). We attempted to further purify the hESC-derived mature neutrophils from the "hESC-Neu" population using density gradient methods, but higher purification could not be achieved without massively reducing the cell yield. We therefore used hESC-Neu's in the subsequent experiments.

Most (97.3% ± 1.5%) of the hESC-derived mature neutrophils defined by Wright-Giemsa staining were positive for myeloperoxidase, and the alkaline-phosphatase score of hESC-Neu's was 284 plus or minus 8.6 (Figure 1B). Under transmission electron microscopy, segmented nuclei and round cytoplasmic granules of hESC-Neu's appeared very similar to those in PB-Neu's (Figure 1C).

Some myeloid cell lines, such as HL-60, have abnormal biosynthesis of secondary granule proteins.[25,26] Thus, it is important to verify the biosynthesis of secondary granule proteins in hESC-Neu's. The levels of lactoferrin mRNA in hESC-derived cells at different stages were compared with those in PB-Neu's and BM-MNCs by semiquantitative RT-PCR (Figure 1D). Lactoferrin biosynthesis begins at the myelocyte stage and terminates by the beginning of the band stage.[25,27] Lactoferrin mRNA was not detected in PB-Neu's from some donors, but was detected in PB-Neu's from others. Human ESC–derived cells at various stages as well as BM-MNCs expressed lactoferrin mRNA. The expression level of lactoferrin mRNA in the hESC-derived cells was highest at day 10 of the induction culture and declined on days 13 and 14. These findings are consistent with the documented pattern of lactoferrin biosynthesis.

Surface antigen presentation in comparison to PB-Neu's

Surface antigen expression at each level of differentiation of hESC-derived cells was analyzed by flow cytometry (Figure 2). From days 7 to 13, the common blood cell antigen CD45 was expressed in almost all the cells. CD34, CD117, and CD133, cell surface markers on normal immature hematopoietic cells, were detected in a small population of the cells on day 7, but disappeared by day 10. Common myeloid antigens CD33 and CD15 were also highly expressed, whereas CD11b expression increased during the course of maturation. CD13 is also a common myeloid antigen, but

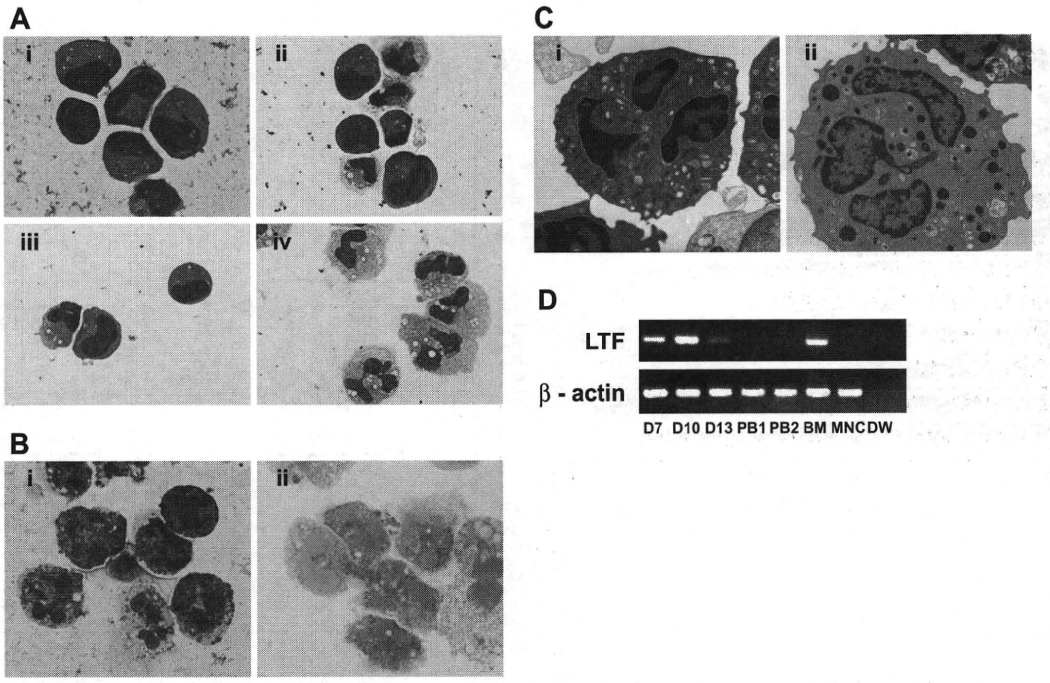

Figure 1. Morphology of hESC-derived cells and expression of lactoferrin mRNA. (A) Wright-Giemsa staining of the day-7 cells (i) revealed that they were morphologically myeloblasts and promyelocytes. On days 9 (ii) and 11 (iii), myelocytes and metamyelocytes were predominant, and on day 13 (iv; hESC-Neu), 70% to 80% of the cells appeared to be stab and segmented neutrophils. Original magnification, ×1000. (Bi) 97.3% plus or minus 1.5% of hESC-Neu's were myeloperoxidase positive. (ii) The neutrophil alkaline-phosphatase score in hESC-Neu's was 284 plus or minus 8.6. Values represent mean plus or minus SD. Original magnification, ×1000. (C) Microstructure of hESC-Neu's. Similar to steady-state neutrophils separated from peripheral blood (i), segmented nuclei and cytoplasmic granules were observed in hESC-Neu's (ii). Original magnification, ×8000. (D) Lactoferrin (LTF) mRNA was expressed in hESC-derived cells on day 7 (D7), peaked on day 10 (D10), and was weakly positive on day 13 (D13). Bone marrow mononuclear cells (BM) were strongly positive for LTF mRNA, but PB-Neu's (PB1 and 2) were negative, although faint bands were detected in PB-Neu's prepared from some donors (data not shown). As a negative control, peripheral blood mononuclear cells (MNCs) were used.

its expression was observed in less than 20% of the cells on day 7 and did not subsequently increase. CD16 (Fcγ receptor (FcγR) III), which is expressed in neutrophils as well as natural killer cells, macrophages, and a small subset of monocytes,[28] was already expressed by day 7, and increased with maturation. This expression pattern of CD16 is consistent with that during normal neutrophil differentiation, although the proportion of $CD16^+$ cells was lower than that of morphology-defined mature neutrophils on day 13. The ratio of CD32 (FcγRII)–positive cells increased as the differentiation stage advanced, and eventually reached 90%. CD64 (FcγRI) expression was greater than 80%, peaking on day 10, and the high percentage was maintained through day 13. CD14 was expressed in 20% to 25% of the cells on days 10 and 13.

Table 1. Differentiation pattern of hESC-derived cells

	% of total cells		
Cell type	Day 7	Day 10	Day 13
Myeloblasts	61.0 ± 9.1	2.3 ± 1.2	ND
Promyelocytes	16.8 ± 6.3	8.5 ± 0.9	0.7 ± 0.8
Myelocytes	12.3 ± 4.8	34.0 ± 6.8	6.4 ± 3.4
Metamyelocytes	3.0 ± 1.0	19.0 ± 1.3	10.2 ± 4.3
Stab neutrophils	0.8 ± 0.3	16.2 ± 3.0	18.3 ± 2.6
Segmented neutrophils	0.3 ± 0.6	14.7 ± 6.0	53.1 ± 9.6
Macrophage/monocytes	5.7 ± 0.6	5.3 ± 1.3	11.2 ± 1.4
Mature neutrophils	1.2 ± 0.8	30.8 ± 4.6	71.4 ± 7.4

The sum of the stab and segmented neutrophils indicates the total mature neutrophils. Data are shown as mean plus or minus SD (n = 3 independent experiments).

ND indicates not detectable.

In normal peripheral blood, both neutrophils and monocytes express CD15 and CD11b. In addition, mature neutrophils express CD16, whereas monocytes express CD14.[28,29] Detailed analysis on day 13 revealed that approximately 70% of $CD15^+$ and $CD11b^+$ cells were $CD16^+$, and almost all $CD15^+$ and $CD16^+$ cells expressed CD11b (Figure 2Bi,ii). Given that 70% to 80% of the cells on day 13 were morphologically mature neutrophils (Table 1), it is likely that the majority of hESC-Neu's had CD15, CD11b, and CD16 expression patterns similar to PB-Neu's, although some hESC-Neu's did not express CD15 or CD16, particularly CD16.

CD32 is broadly expressed on myeloid cells, whereas CD64 is expressed only on monocytes but not on neutrophils in the peripheral blood.[28] In the bone marrow, CD64 expression is observed in a small population of myeloblasts, peaks at the promyelocyte, myelocyte, and metamyelocyte stages, and then diminishes, although a small proportion of the stab neutrophils still express CD64.[30,31] We confirmed that virtually no PB-Neu's expressed CD64 (data not shown). In contrast, almost all $CD15^+$ and $CD16^+$ hESC-Neu's expressed CD64 on day 13, indicating that both stab and segmented hESC-Neu's expressed CD64, because segmented neutrophils represented more than 50% of the cells on day 13 (Figure 2Biii; Table 1). Nearly 50% of $CD15^+$ and $CD16^+$ cells were weakly positive for CD14, in contrast to the negative expression of CD14 in steady-state PB-Neu's (Figure 2Biv). This aberrant expression of CD64 and CD14 in hESC-Neu's is similar to their positive expression on some of the neutrophils harvested from healthy donors who received G-CSF administration[32,33] and the neutrophils derived from bone marrow $CD34^+$ cells in vitro by G-CSF stimulation.[31]

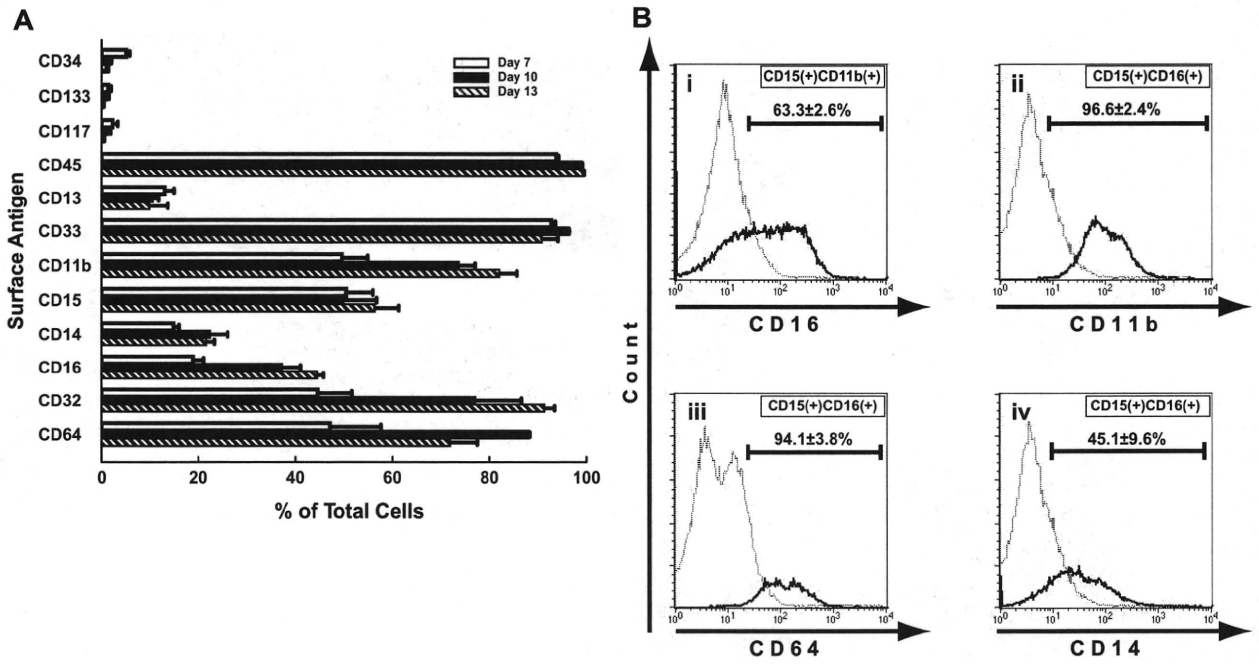

Figure 2. Surface antigens of hESC-derived cells. (A) Surface antigen expression at each level of differentiation of hESC-derived cells was analyzed by flow cytometry. CD45 was expressed in almost all the cells. CD34, CD117, and CD133, immature markers of hematopoiesis, were detected in a small population of the cells on day 7, and had almost disappeared by day 10. Common myeloid antigens CD33 and CD15 were highly expressed, and the expression of CD11b increased during maturation. CD13 was expressed in less than 20% of the cells throughout the culture period. The expression of CD16, a mature neutrophil marker, increased following maturation, but was observed in only approximately 45% of the cells, even on day 13. CD14 and CD64 expression was aberrantly observed in some cells. Bars represent SDs (n = 3). (B) In the steady state, mature neutrophils in peripheral blood were $CD15^+$, $CD11b^+$, and $CD16^+$. (i) In hESC-derived cells on day 13, 63.3% plus or minus 2.6% of the $CD15^+$ and $CD11b^+$ cells were $CD16^+$, and (ii) almost all of the $CD15^+$ and $CD16^+$ cells were $CD11b^+$. (iii-iv) On the other hand, CD64 and CD14 were rarely expressed on mature neutrophils in the peripheral blood. $CD15^+$ and $CD16^+$ cells from hESCs, consistent with the phenotype of mature neutrophils, showed aberrant expression of CD64 (iii) and CD14 (iv), in 94.1% plus or minus 3.8% and 45.1% plus or minus 9.6% of the cells, respectively. Data are presented as mean plus or minus SD (n = 3).

Apoptosis pattern and prolonged survival by G-CSF of hESC-Neu's and PB-Neu's

In the steady state, PB-Neu's have a short life span of approximately 24 hours, but this can be prolonged by G-CSF stimulation.[34] Some hESC-Neu's were already apoptotic at the time of harvest and therefore we focused on the nonapoptotic fraction of hESC-Neu's (Figure 3). In contrast to the PB-Neu's, which underwent apoptosis within 6 hours without G-CSF, consistent with previous reports,[34] a proportion of apoptotic cells among hESC-Neu's in the medium without G-CSF did not increase for up to 6 hours after the start of the culture. In addition, there were no differences between the cultures with and without G-CSF for up to 6 hours. After 6 hours, however, there was a more rapid decrease in nonapoptotic cells in hESC-Neu's without G-CSF than in hESC-Neu's with G-CSF, which resulted in a lower number of viable cells than hESC-Neu's with G-CSF at 24 hours, although the number of viable cells of hESC-Neu's without G-CSF was still higher than that of PB-Neu's without G-CSF.

Oxidative burst phenotype was similar in hESC-Neu's and PB-Neu's

Oxidative burst is an essential function of neutrophils when killing microorganisms, but an inappropriate burst sometime causes injury to the host tissue. We assessed the ability to convert DHR to rhodamine in hESC-Neu's and PB-Neu's using flow cytometry.[20] Because G-CSF, which could substantially affect the result, was used during the culture, we compared hESC-Neu's with PB-Neu(G+)'s and PB-Neu(G−)'s as described in "G-CSF stimulation prior to assessing neutrophil function." When DHR was added to the neutrophil suspensions, rhodamine-specific fluorescence was detected in hESC-Neu's, and in PB-Neu(G−)'s and PB-Neu(G+)'s without PMA stimulation, indicating basal superoxide production without PMA stimulation in each neutrophil preparation (Figure 4). PMA stimulation increased rhodamine mean fluorescence intensity in hESC-Neu's, but to a lesser extent than in PB-Neu(G−)'s and PB-Neu(G+)'s. Consequently, the mean rhodamine fluorescence intensity after PMA stimulation was similar in hESC-Neu's, PB-Neu(G−)'s, and PB-Neu(G+)'s, suggesting that the maximum superoxide production is comparable between hESC-Neu's and PB-Neu's.

Phagocytosis and subsequent NBT reduction activity, and bactericidal activity were similar between hESC-Neu's and PB-Neu's

Neutrophils protect against infectious microorganisms by phagocytosing and subsequently killing them. These functions of hESC-Neu's and PB-Neu's were evaluated in an experimental system using NBT-coated yeast. Under the microscope, mature neutrophils could be easily distinguished from contaminating macrophages by the unique shape of their nuclei after 1% safranin-O staining (Figure 5A). NBT-coated yeast that had not been ingested had a red-brown color that began to change to purple or black, beginning at the periphery, and eventually became completely black, because the NBT coating on the yeast was reduced by neutrophils after phagocytosis. Thus, neutrophils that had phagocytosis and NBT-reducing ability could be easily identified. hESC-Neu's had a slightly lower phagocytosis rate than PB-Neu(G−)'s and PB-Neu(G+)'s (Figure 5B). The phagocytosis score, however, was not significantly different between hESC-Neu's and PB-Neu(G−)'s and PB-Neu(G+)'s (Figure 5C). The cells on day 8 of the culture, most of which were morphologically myeloblasts and promyelocytes, were rarely observed

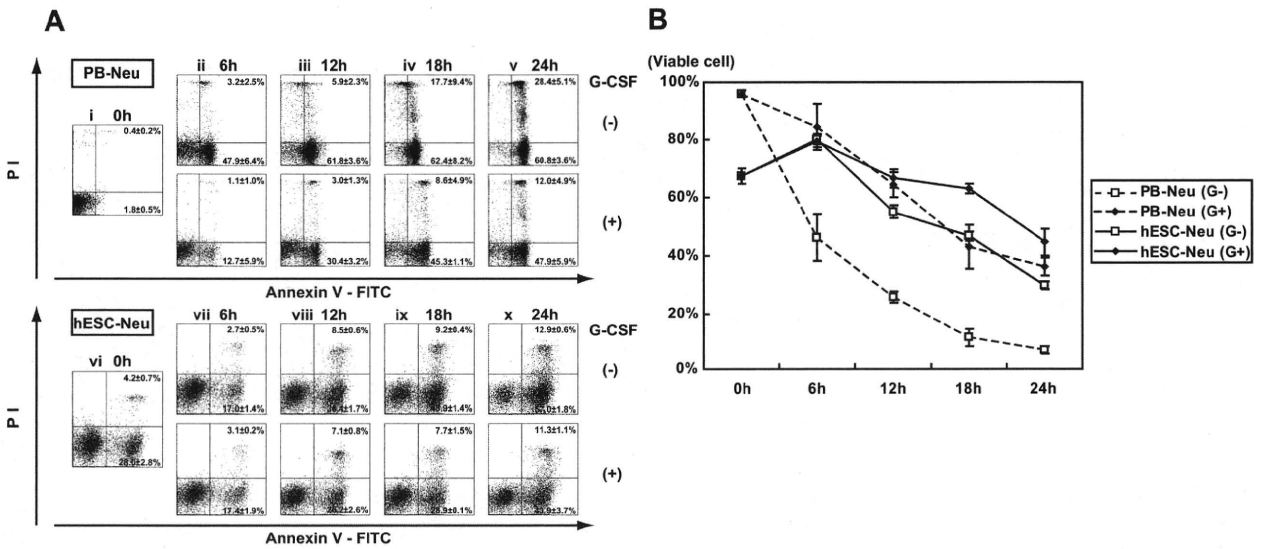

Figure 3. Apoptosis pattern and G-CSF effect on survival of hESC-Neu's. (A) Flow cytometric analysis. In the steady state, PB-Neu's have a short life span of approximately 24 hours, but this can be prolonged by G-CSF stimulation (i-v). Some hESC-Neu's were already apoptotic at the time of the harvest from the induction culture (vi). In contrast to the PB-Neu's that underwent apoptosis within 6 hours without G-CSF (ii), the proportion of apoptotic cells did not increase for up to 6 hours after the start of the culture of hESC-Neu's in the medium without G-CSF (vi,vii). In addition, there were no differences between the cultures of hESC-Neu's with and without G-CSF for up to 6 hours (vii). After 6 hours, nonapoptotic cells decreased more rapidly among hESC-Neu's without G-CSF than among hESC-Neu's with G-CSF (viii-x), resulting in the lower number of viable cells than hESC-Neu's with G-CSF at 24 hours (x). Figures are representative of 3 independent experiments. Data are presented as mean plus or minus SD (n = 3). (B) The time course of the decrease in viable cells. Bars represent SDs (n = 3).

to phagocytose the yeast or reduce NBT if they had ingested the yeast, indicating that we observed phagocytosis and NBT reduction that was specific to mature neutrophils.

Because the hESC-Neu's had sufficient phagocytosing ability and superoxide production, we next investigated whether hESC-Neu's can kill bacteria. The bactericidal activity of hESC-Neu's and PB-Neu's was compared using *E coli*. When incubated with hESC-Neu's and PB-Neu(G−)'s and PB-Neu(G+)'s, the numbers of CFUs were similarly reduced to approximately 40% that of the control, indicating comparable bactericidal activity against *E coli* between hESC-Neu's and PB-Neu's (Figure 5D).

Chemotaxis was similar between hESC-Neu's and PB-Neu's

We compared chemotaxis of hESC-Neu's and PB-Neu's using a modified Boyden chamber method. After incubation with or without fMLP in the lower well, neutrophils had migrated from the upper side to the lower side of the membrane. Neutrophil migration without fMLP in the lower well was considered random migration. The number of neutrophils that migrated randomly was not significantly different between hESC-Neu's and PB-Neu(G−)'s, but PB-Neu(G+)'s showed significantly more random migration than the others (Figure 5E). The number of migrated cells increased in hESC-Neu's, PB-Neu(G−)'s, and PB-Neu(G+)'s when fMLP was added in the lower well. The increase in cell migration induced by chemotaxis to fMLP was calculated by subtracting the number of randomly migrated cells without fMLP from that of migrated cells with fMLP. There were no significant differences between hESC-Neu's and PB-Neu(G−)'s or PB-Neu(G+)'s in the net fMLP-induced chemotaxis.

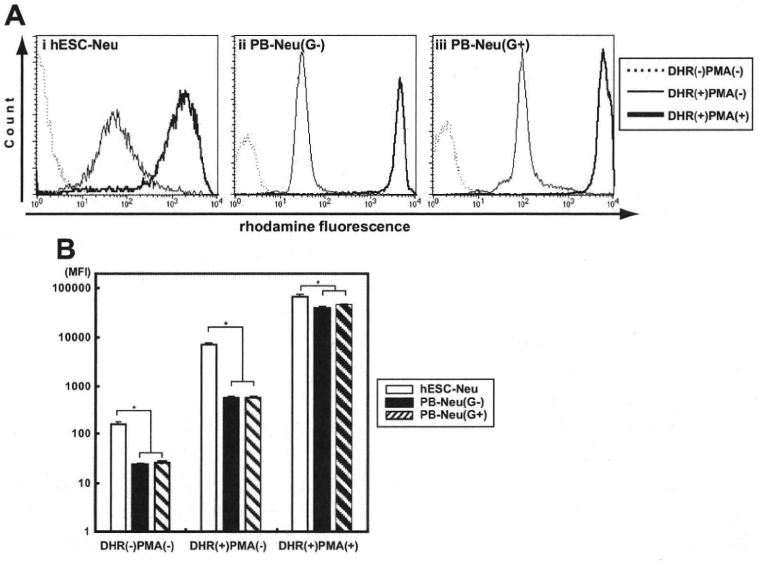

Figure 4. Superoxide production of hESC-Neu's assessed by dihydrorhodamine123 oxidation. (A) Dihydrorhodamine123 (DHR) was reacted to neutrophils with or without phorbol myristate acetate (PMA), and the resultant rhodamine fluorescence was detected by flow cytometry. When DHR was added to the reaction medium without PMA (line), the fluorescence levels were slightly elevated in hESC-Neu's (i), PB-Neu(G−)'s (ii), and PB-Neu(G+)'s (iii). The addition of PMA dramatically increased the levels of fluorescence in all 3 neutrophil preparations (bold line). The figures are representative of 3 independent experiments. (B) Comparison of superoxide production between hESC-Neu's and PB-Neu's using mean fluorescence intensity (MFI) of rhodamine. When DHR was added without PMA stimulation, rhodamine-specific fluorescence was detected in hESC-Neu's, PB-Neu(G−)'s, and PB-Neu(G+)'s. PMA stimulation increased rhodamine MFI in hESC-Neu's though to a lesser extent than in PB-Neu(G−)'s and PB-Neu(G+)'s. Consequently, rhodamine MFI after PMA stimulation was similar in hESC-Neu's, PB-Neu(G−)'s, and PB-Neu(G+)'s, suggesting that the maximum superoxide production was comparable between hESC-Neu's and PB-Neu's (n = 3; bars represent SDs; $^*P < .05$ compared with hESC-Neu's).

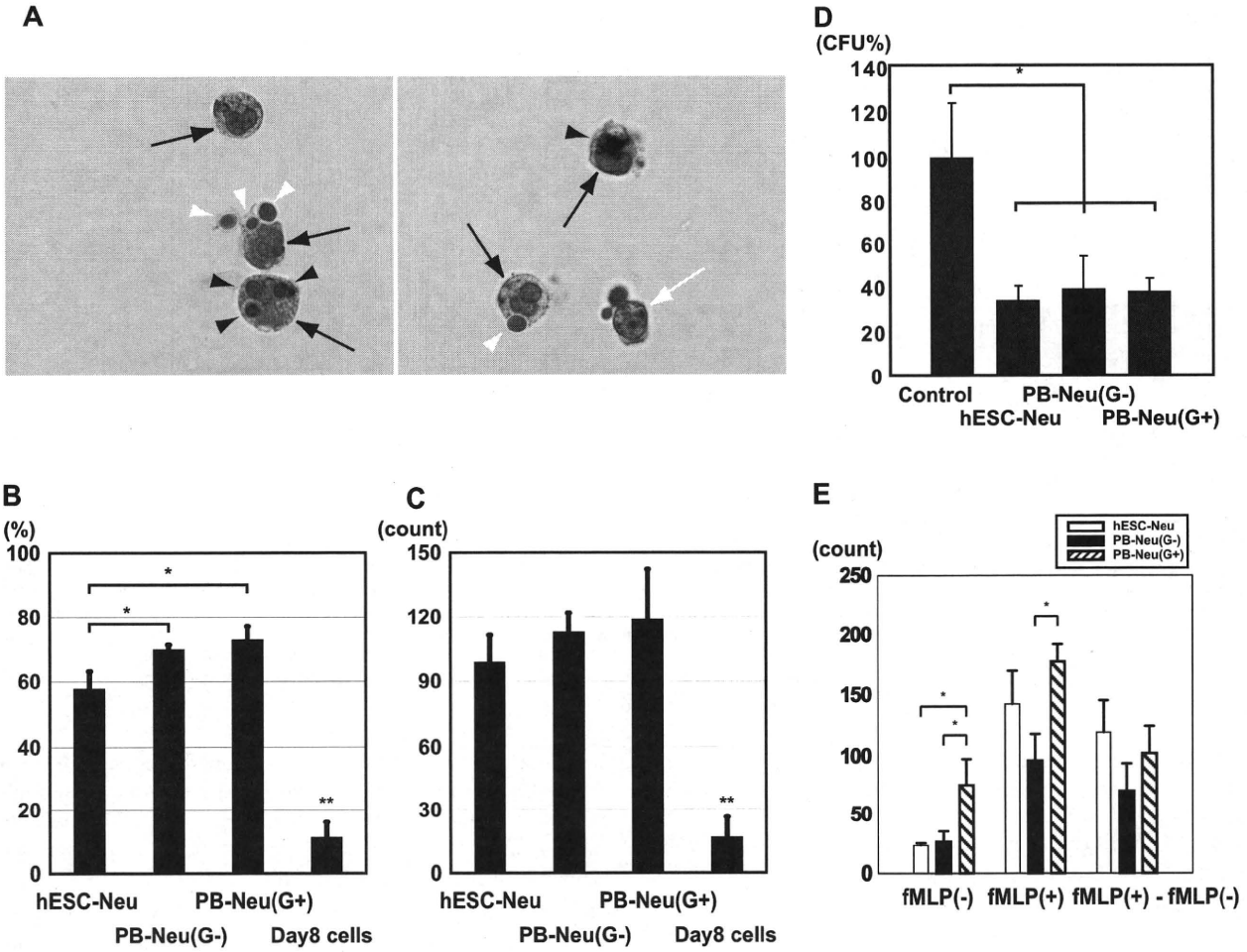

Figure 5. NBT-coated yeast cell-phagocytosis test, bactericidal activity, and chemotaxis assay. (A) NBT-coated yeast cells were added to a neutrophil suspension and incubated at 37°C. After 1 hour, the cells were stained with 1% safranin-O, and observed using a microscope. Mature neutrophils (→) could be easily distinguished from contaminating macrophages (white arrow; only the nucleus is observed in the figure) by the unique shape of their nuclei. Yeast cells were red-brown in color before being ingested (white arrowhead); the color began to change to purple or black beginning at the periphery of the yeast cell, and eventually became completely black (➤) because the NBT was reduced after ingestion. Yeast cells that changed color in the cells were counted as NBT-reduction positive. Original magnification, ×400. (B) The phagocytosis rate was calculated as a percentage of the neutrophils that contained one or more yeast cells. hESC-Neu's had a slightly lower phagocytosis rate than that of PB-Neu(G−)'s and PB-Neu(G+)'s. (C) The phagocytosis score was calculated as the total number of positive yeast cells in 100 neutrophils. There were no significant differences in the phagocytosis score between hESC-Neu's and PB-Neu(G−)'s or PB-Neu(G+)'s. The cells on day 8 of the culture (day-8 cells) were rarely observed to phagocytose the yeast cells or reduce NBT. (In B-C, n = 3; bars indicate SDs; $*P < .05$ compared with PB-Neu(G−)'s and PB-Neu(G+)'s; $**P < .05$ compared with hESC-Neu's, PB-Neu(G−)'s, and PB-Neu(G+)'s.) (D) Bactericidal assay. *E coli* was opsonized with human AB serum, and incubated with hESC-Neu's, PB-Neu(G−)'s, PB-Neu(G+)'s, or control medium. After 1-hour incubation with hESC-Neu's, PB-Neu(G−)'s, and PB-Neu(G+)'s, the colony-forming units (CFUs) were significantly reduced to approximately 40% of the control. There were no significant differences in bactericidal activity between hESC-Neu's, PB-Neu(G−)'s, and PB-Neu(G+)'s. The CFUs of controls are presented as 100% (n = 3; bars indicate SDs; $*P < .05$ compared with control). (E) Chemotaxis assay by a modified Boyden chamber method. The number of neutrophils that migrated randomly (fMLP(−)) was not significantly different between hESC-Neu's and PB-Neu(G−)'s, but PB-Neu(G+)'s showed significantly greater random migration than hESC-Neu's and PB-Neu(G−)'s. The number of migrating cells increased in all hESC-Neu's, PB-Neu(G−)'s, and PB-Neu(G+)'s when fMLP was added to the lower well (fMLP(+)). The increase in the number of migrating cells induced by chemotaxis to fMLP (fMLP(+)-fMLP(−)) was not significantly different between hESC-Neu's and PB-Neu(G−)'s or PB-Neu(G+)'s (n = 3; bars indicate SDs; $*P < .05$).

Discussion

We developed a specific and effective method for deriving mature neutrophils from hESCs, making it possible to analyze hESC-derived neutrophils in detail. hESC-derived neutrophils had characteristics similar to steady-state peripheral blood mature neutrophils in morphology and essential functions, although there were some differences in surface antigen expression.

Unfortunately, attempts to further purify the hESC-derived mature neutrophils from the hESC-Neu population by density gradient methods led to a massive reduction in cell yield. In the flow cytometric analysis, the mean intensity of hESC-Neu's in forward scatter was higher than that of PB-Neu's (data not shown), indicating that the size of morphologically mature neutrophils, comprising 70% to 80% of the hESC-Neu population, was larger than that of PB-Neu's. This finding indicates that the density of morphologically mature neutrophils in the hESC-Neu population was lower than that of PB-Neu's, which made it difficult to separate hESC-Neu's from other contaminating cells.

In this culture, we observed morphologically defined myeloblasts, promyelocytes, myelocytes, metamyelocytes, and, eventually, mature stab and segmented neutrophils, in this order, during the 13-day culture, which is similar to the granulocyte maturation process in bone marrow. The surface antigen expression pattern during differentiation was similar to that during normal granulopoiesis, with CD34 and CD117 expression on immature cells, and an increase in CD16 expression as differentiation advanced. Most

hESC-Neu's expressed CD16, CD15, CD11b, CD33, and CD45. This pattern is consistent with normal PB-Neu's, but the percentage of CD16-expressing cells was lower than that of mature neutrophils determined by morphology. The lower CD16 expression level is documented in neutrophils derived in vitro from bone marrow $CD34^+$ cells by stimulation with G-CSF, and is considered to be the effect of G-CSF on myeloid progenitors.[31] G-CSF also induces CD64 and CD14 expression on mature neutrophils,[31,35] and these effects are also observed in vivo when G-CSF is administered to healthy volunteers.[32,33] Therefore, the G-CSF present in the culture from day 7 may have affected the progenitors and led to the relatively low expression of CD16 on hESC-Neu's and aberrant expression of CD64 and CD14 on $CD15^+$ and $CD16^+$ hESC-Neu's.

In the apoptosis assay, some hESC-Neu's were already apoptotic at the time of the harvest from the induction culture, but the proportion of apoptotic cells among hESC-Neu's in the medium without G-CSF did not increase for up to 6 hours after the start of the culture. There are 2 possible reasons for the difference in the rate of apoptosis. First, the hESC-Neu's were more heterogeneous than the PB-Neu's, as they comprised cells at different stages from incompletely differentiated cells such as metamyelocytes to maturation-completed and aged neutrophils. Relatively immature cells or unaged mature neutrophils in the hESC-Neu population might have a longer lifespan than PB-Neu's. Second, the effect of G-CSF used in the induction culture might continue even after the washout.

In the chemotaxis assay, the random migration of hESC-Neu's was almost the same as that of PB-Neu(G−)'s, but lower than that of PB-Neu(G+)'s, although hESC-Neu's were stimulated by G-CSF before the assay. The effect of G-CSF on the random migration of neutrophils is controversial; random migration increases in vitro when neutrophils are stimulated by G-CSF,[36] whereas neutrophils obtained from G-CSF–treated patients with nonmyeloid malignancies show decreased random migration and chemotaxis.[37,38] Our in vitro experiment with PB-Neu(G+)'s and PB-Neu(G−)'s replicated the former result. Nevertheless, hESC-Neu's showed relatively low random migration despite stimulation with G-CSF, while maintaining almost normal fMLP-induced chemotaxis. One possible reason for these differences might be the continuous stimulation by G-CSF; hESC-Neu's were stimulated from the myeloblast stage, and thus, it was expected that the characteristics of the hESC-Neu's were more similar to those of neutrophils from G-CSF–stimulated donors rather than to normal mature neutrophils.

The low yield of hESC-Neu's is a major obstacle to their functional analysis in animals, and further, to their potential use in drug screening and clinical applications. The number of hESC-Neu's produced was less than twice that of the input EB-derived cells. Recently, erythroid progenitor cell lines that could differentiate into functional mature red blood cells both in vitro and in vivo were established from mouse ESCs.[39] In that report, the starting number of ESCs required to establish one progenitor line was 5×10^5, and transplantation of 2×10^7 cells of the progenitor line could ameliorate anemia in mice by increasing the red blood cell count. Similar methods could be considered in the granulopoiesis from hESCs. Another potential method is to use more immature or proliferation-competent cells than the cells with which we initiated the induction culture. One candidate may be hematopoietic progenitors that emerge in saclike structures derived from ESCs. In a report using cynomolgus monkey ESCs,[40] EBs were created and subsequently subjected to adherent culture on a gelatin-coated dish. After 2 weeks, saclike structures emerged that contained hematopoietic precursors at various stages of myeloid lineage. The authors mentioned the possible existence of hemangioblasts, because endothelial cells could be produced from those precursors under different conditions. Others have also reported similar saclike structures containing hematopoietic precursors created from hESCs.[10] In this paper, megakaryocytes were created from the inner cells, which were positive for hematoendothelial markers, such as CD34, CD31, vascular endothelial growth factor-receptor 2, and vascular endothelial-cadherin. These similar findings suggest that the cells in the saclike structures contain cells that are more immature than our EB-derived cells, and that the precursors inside the saclike structures have greater proliferation potency than our EB-derived cells. Because neither paper directly demonstrated the efficiency of mature blood cell production from monkey or human ES cells, however, the efficiency of producing neutrophils from our EB-derived cells should be compared with that from the saclike structure–derived cells.

Acknowledgments

We thank Dr Nakatsuji for providing the KhES-3, and Dr Nakano for providing the OP9 cells. We are grateful to Kyowa Hakko Kirin for providing TPO, FP6, and G-CSF, and to Kyokuto Pharmaceutical Industrial for the nonserum medium used in the EB formation. We also thank S. Ichimura for hESC culture.

This work was supported in part by a Grant-in-aid from the Japan Society of Promotion of Sciences (KAKENHI nos. 17390274, 18013012, 19390258, and 20015010); Research on Pharmaceutical and Medical Safety, Health and Labor Sciences Research Grants from the Ministry of Health, Labor and Welfare of Japan (H16-Iyaku-32); grants from the Astellas Foundation for Research on Metabolic Disorders; the Uehara Memorial Foundation; and the Sagawa Foundation for Promotion of Cancer Research (S.C.); and the Project for Realization of Regenerative Medicine (S.O.).

Authorship

Contribution: Y.Y. and T.S. performed the experiments; K.H. designed the NBT-coated yeast cell-phagocytosis test; M.S.-Y., and K.K. assisted with interpretation of experiments and provided insightful comments; Y.Y. interpreted the data, made the figures, and wrote the paper; T.T., M.K., and S.O. advised on experimental design; S.C. provided critical reading of the paper; T.S. and S.C. designed the research.

Conflict-of-interest disclosure: The authors declare no competing financial interests.

Correspondence: Shigeru Chiba, Department of Clinical and Experimental Hematology, University of Tsukuba, 1-1-1 Tennodai, Tsukuba, Ibaraki, 305-8575, Japan; e-mail: schiba-tky@umin.net.

References

1. Kaufman DS, Hanson ET, Lewis RL, Auerbach R, Thomson JA. Hematopoietic colony-forming cells derived from human embryonic stem cells. Proc Natl Acad Sci U S A. 2001;98:10716-10721.
2. Nakano T, Kodama H, Honjo T. Generation of lymphohematopoietic cells from embryonic stem cells in culture. Science. 1994;265:1098-1101.
3. Vodyanik MA, Bork JA, Thomson JA, Slukvin II. Human embryonic stem cell-derived CD34+ cells: efficient production in the coculture with OP9 stromal cells and analysis of lymphohematopoietic potential. Blood. 2005;105:617-626.

4. Chadwick K, Wang L, Li L, et al. Cytokines and BMP-4 promote hematopoietic differentiation of human embryonic stem cells. Blood. 2003;102: 906-915.
5. Cerdan C, Rouleau A, Bhatia M. VEGF-A165 augments erythropoietic development from human embryonic stem cells. Blood. 2004;103: 2504-2512.
6. Wang L, Menendez P, Shojaei F, et al. Generation of hematopoietic repopulating cells from human embryonic stem cells independent of ectopic HOXB4 expression. J Exp Med. 2005;201:1603-1614.
7. Keller G, Kennedy M, Papayannopoulou T, Wiles MV. Hematopoietic commitment during embryonic stem cell differentiation in culture. Mol Cell Biol. 1993;13:473-486.
8. Wang L, Li L, Shojaei F, et al. Endothelial and hematopoietic cell fate of human embryonic stem cells originates from primitive endothelium with hemangioblastic properties. Immunity. 2004;21: 31-41.
9. Lu SJ, Feng Q, Caballero S, et al. Generation of functional hemangioblasts from human embryonic stem cells. Nat Methods. 2007;4:501-509.
10. Takayama N, Nishikii H, Usui J, et al. Generation of functional platelets from human embryonic stem cells in vitro via ES-sacs, VEGF-promoted structures that concentrate hematopoietic progenitors. Blood. 2008;111:5298-5306.
11. Hübel K, Carter RA, Liles WC, et al. Granulocyte transfusion therapy for infections in candidates and recipients of HPC transplantation: a comparative analysis of feasibility and outcome for community donors versus related donors. Transfusion. 2002;42:1414-1421.
12. Mousset S, Hermann S, Klein SA, et al. Prophylactic and interventional granulocyte transfusions in patients with haematological malignancies and life-threatening infections during neutropenia. Ann Hematol. 2005;84:734-741.
13. Price TH. Granulocyte transfusion: current status. Semin Hematol. 2007;44:15-23.
14. Bhatia M. Hematopoietic development from human embryonic stem cells. Hematology Am Soc Hematol Educ Program. 2007;2007:11-16.
15. Suemori H, Yasuchika K, Hasegawa K, Fujioka T, Tsuneyoshi N, Nakatsuji N. Efficient establishment of human embryonic stem cell lines and long-term maintenance with stable karyotype by enzymatic bulk passage. Biochem Biophys Res Commun. 2006;345:926-932.
16. Thomson JA, Itskovitz-Eldor J, Shapiro SS, et al. Embryonic stem cell lines derived from human blastocysts. Science. 1998;282:1145-1147.
17. Suzuki T, Yokoyama Y, Kumano K, et al. Highly efficient ex vivo expansion of human hematopoietic stem cells using Delta1-Fc chimeric protein. Stem Cells. 2006;24:2456-2465.
18. Yuo A, Kitagawa S, Okabe T, et al. Recombinant human granulocyte colony-stimulating factor repairs the abnormalities of neutrophils in patients with myelodysplastic syndromes and chronic myelogenous leukemia. Blood. 1987;70:404-411.
19. Kumano K, Chiba S, Shimizu K, et al. Notch1 inhibits differentiation of hematopoietic cells by sustaining GATA-2 expression. Blood. 2001;98:3283-3289.
20. Vowells SJ, Sekhsaria S, Malech HL, Shalit M, Fleisher TA. Flow cytometric analysis of the granulocyte respiratory burst: a comparison study of fluorescent probes. J Immunol Methods. 1995; 178:89-97.
21. Richardson MP, Ayliffe MJ, Helbert M, Davies EG. A simple flow cytometry assay using dihydrorhodamine for the measurement of the neutrophil respiratory burst in whole blood: comparison with the quantitative nitrobluetetrazolium test. J Immunol Methods. 1998;219:187-193.
22. Emmendörffer A, Hecht M, Lohmann-Matthes ML, Roesler J. A fast and easy method to determine the production of reactive oxygen intermediates by human and murine phagocytes using dihydrorhodamine 123. J Immunol Methods. 1990; 131:269-275.
23. Decleva E, Menegazzi R, Busetto S, Patriarca P, Dri P. Common methodology is inadequate for studies on the microbicidal activity of neutrophils. J Leukoc Biol. 2006;79:87-94.
24. Harvath L, Falk W, Leonard EJ. Rapid quantitation of neutrophil chemotaxis: use of a polyvinylpyrrolidone-free polycarbonate membrane in a multiwell assembly. J Immunol Methods. 1980;37: 39-45.
25. Rado TA, Bollekens J, St Laurent G, Parker L, Benz EJ Jr. Lactoferrin biosynthesis during granulocytopoiesis. Blood. 1984;64:1103-1109.
26. Rado TA, Wei XP, Benz EJ Jr. Isolation of lactoferrin cDNA from a human myeloid library and expression of mRNA during normal and leukemic myelopoiesis. Blood. 1987;70:989-993.
27. Cowland JB, Borregaard N. The individual regulation of granule protein mRNA levels during neutrophil maturation explains the heterogeneity of neutrophil granules. J Leukoc Biol. 1999;66:989-995.
28. van de Winkel JG, Anderson CL. Biology of human immunoglobulin G Fc receptors. J Leukoc Biol. 1991;49:511-524.
29. van Lochem EG, van der Velden VH, Wind HK, te Marvelde JG, Westerdaal NA, van Dongen JJ. Immunophenotypic differentiation patterns of normal hematopoiesis in human bone marrow: reference patterns for age-related changes and disease-induced shifts. Cytometry B Clin Cytom. 2004;60:1-13.
30. Ball ED, McDermott J, Griffin JD, Davey FR, Davis R, Bloomfield CD. Expression of the three myeloid cell-associated immunoglobulin G Fc receptors defined by murine monoclonal antibodies on normal bone marrow and acute leukemia cells. Blood. 1989;73:1951-1956.
31. Kerst JM, van de Winkel JG, Evans AH, et al. Granulocyte colony-stimulating factor induces hFc gamma RI (CD64 antigen)-positive neutrophils via an effect on myeloid precursor cells. Blood. 1993;81:1457-1464.
32. Kerst JM, de Haas M, van der Schoot CE, et al. Recombinant granulocyte colony-stimulating factor administration to healthy volunteers: induction of immunophenotypically and functionally altered neutrophils via an effect on myeloid progenitor cells. Blood. 1993;82:3265-3272.
33. Carulli G. Effects of recombinant human granulocyte colony-stimulating factor administration on neutrophil phenotype and functions. Haematologica. 1997;82:606-616.
34. van Raam BJ, Drewniak A, Groenewold V, van den Berg TK, Kuijpers TW. Granulocyte colony-stimulating factor delays neutrophil apoptosis by inhibition of calpains upstream of caspase-3. Blood. 2008;112:2046-2054.
35. Kerst JM, Slaper-Cortenbach IC, von dem Borne AE, van der Schoot CE, van Oers RH. Combined measurement of growth and differentiation in suspension cultures of purified human CD34-positive cells enables a detailed analysis of myelopoiesis. Exp Hematol. 1992;20:1188-1193.
36. Nakamae-Akahori M, Kato T, Masuda S, et al. Enhanced neutrophil motility by granulocyte colony-stimulating factor: the role of extracellular signal-regulated kinase and phosphatidylinositol 3-kinase. Immunology. 2006;119:393-403.
37. Azzarà A, Carulli G, Rizzuti-Gullaci A, Minnucci S, Capochiani E, Ambrogi F. Motility of rhG-CSF-induced neutrophils in patients undergoing chemotherapy: evidence for inhibition detected by image analysis. Br J Haematol. 1996;92:161-168.
38. Ribeiro D, Veldwijk MR, Benner A, et al. Differences in functional activity and antigen expression of granulocytes primed in vivo with filgrastim, lenograstim, or pegfilgrastim. Transfusion. 2007; 47:969-980.
39. Hiroyama T, Miharada K, Sudo K, Danjo I, Aoki N, Nakamura Y. Establishment of mouse embryonic stem cell-derived erythroid progenitor cell lines able to produce functional red blood cells. PLoS ONE. 2008;3:e1544.
40. Nakahara M, Matsuyama S, Saeki K, et al. A feeder-free hematopoietic differentiation system with generation of functional neutrophils from feeder- and cytokine-free primate embryonic stem cells. Cloning Stem Cells. 2008;10:341-354.

Notch Activation Induces the Generation of Functional NK Cells from Human Cord Blood CD34-Positive Cells Devoid of IL-15[1]

Kyoko Haraguchi,*† Takahiro Suzuki,[2]*‡ Noriko Koyama,‖ Keiki Kumano,*‡ Fumio Nakahara,[3]*‡ Akihiko Matsumoto,[4]* Yasuhisa Yokoyama,[5]*‡ Mamiko Sakata-Yanagimoto,[5]*‡ Shigeo Masuda,[6]*‡ Tsuyoshi Takahashi,‡ Aki Kamijo,[7]§ Koki Takahashi,§ Minoko Takanashi,# Yoshiki Okuyama,† Koji Yasutomo,** Seiji Sakano,†† Hideo Yagita,‖ Mineo Kurokawa,‡ Seishi Ogawa,‡¶ and Shigeru Chiba[8]*‡‡

The development of NK cells from hematopoietic stem cells is thought to be dependent on IL-15. In this study, we demonstrate that stimulation of human cord blood CD34$^+$ cells by a Notch ligand, Delta4, along with IL-7, stem cell factor, and Fms-like tyrosine kinase 3 ligand, but no IL-15, in a stroma-free culture induced the generation of cells with characteristics of functional NK cells, including CD56 and CD161 Ag expression, IFN-γ secretion, and cytotoxic activity against K562 and Jurkat cells. Addition of γ-secretase inhibitor and anti-human Notch1 Ab to the culture medium almost completely blocked NK cell emergence. Addition of anti-human IL-15-neutralizing Ab did not affect NK cell development in these culture conditions. The presence of IL-15, however, augmented cytotoxicity and was required for a more mature NK cell phenotype. CD56$^+$ cells generated by culture with IL-15, but without Notch stimulation, were negative for CD7 and cytoplasmic CD3, whereas CD56$^+$ cells generated by culture with both Delta4 and IL-15 were CD7$^+$ and cytoplasmic CD3$^+$ from the beginning and therefore more similar to in vivo human NK cell progenitors. Together, these results suggest that Notch signaling is important for the physiologic development of NK cells at differentiation stages beyond those previously postulated. *The Journal of Immunology,* **2009, 182: 6168–6178.**

Natural killer cells are critical for host immunity because they rapidly mediate cellular cytotoxicity against pathogen-infected or malignantly transformed cells and produce a wide variety of cytokines and chemokines that influence other components of the immune system. Unlike other lymphocytic lineages, however, the continuous staging scheme of human NK cell development in vivo has yet to be elucidated (1). One reason for this may be the difficulty in closely correlating our knowledge of mouse NK cell biology with human NK cell biology (2), because mouse NK cells do not express a homolog of CD56, which is the marker most representative of human NK cells; instead, the most widely used markers of NK cells in various mouse strains are NK1.1 and DX5, mouse-specific Ags. Among the molecules involved in NK cell development, IL-15 has a particularly important role. For example, IL-15-deficient mice lack NK1.1$^+$ cells (3), indicating that IL-15 is essential for NK cell development in mice. The requirement of IL-15 for mouse NK cell development has also been demonstrated by other studies (4, 5). In humans, IL-15 is considered to be required for in vitro NK cell development and virtually most current protocols for human NK cell differentiation culture depend on IL-15. IL-15-independent NK cell differentiation has been reported in which human cord blood (CB)[9] cells are cocultured with murine stromal cell lines (6). Signaling, however, substituting IL-15 signaling that is responsible for the NK cell differentiation in this culture system was not described.

NK cells are thought to be derived from hematopoietic stem cells through a T/NK precursor stage. The Notch signaling pathway influences cell fate decisions in numerous cellular systems,

*Department of Cell Therapy and Transplantation Medicine, University of Tokyo Hospital, Tokyo, Japan; †Division of Transfusion and Cell Therapy, Tokyo Metropolitan Cancer and Infectious Disease Center Komagome Hospital, Tokyo, Japan; ‡Department of Hematology and Oncology, Graduate School of Medicine, §Department of Transfusion Medicine, Graduate School of Medicine, and ¶21th Century Center of Excellence Program, University of Tokyo, Tokyo, Japan; ‖Department of Immunology, Juntendo University School of Medicine, Tokyo, Japan; #Tokyo Metropolitan Red Cross Blood Center, Tokyo, Japan; **Department of Immunology, Graduate School of Biomedical Sciences, Tokushima University, Tokushima, Japan; ††Corporate R&D Laboratory, Asahi Kasei Corporation, Tokyo, Japan; and ‡‡Department of Clinical and Experimental Hematology, Graduate School of Comprehensive Human Sciences, University of Tsukuba, Ibaraki, Japan

Received for publication September 17, 2008. Accepted for publication March 9, 2009.

The costs of publication of this article were defrayed in part by the payment of page charges. This article must therefore be hereby marked *advertisement* in accordance with 18 U.S.C. Section 1734 solely to indicate this fact.

[1] This work was supported in part by the Research on Pharmaceutical and Medical Safety, Health and Labor Sciences Research Grants from the Ministry of Health, Labor and Welfare of Japan (H16-Iyaku-32) and grants from the Astellas Foundation for Research on Metabolic Disorders, the Uehara Memorial Foundation, and the Sagawa Foundation for Promotion of Cancer Research (to S.C.). K.H. was supported by a fellowship from the Society of Japanese Pharmacopoeia.

[2] Current address: Department of Hematology, Jichi Medical University, Tochigi, Japan.

[3] Current address: Division of Cellular Therapy, Advanced Clinical Research Center, Institute of Medical Science, University of Tokyo, Tokyo, Japan.

[4] Current address: Department of Urology, Tokyo Metropolitan Bokutoh Hospital, Tokyo, Japan.

[5] Current address: Department of Clinical and Experimental Hematology, University of Tsukuba, Ibaraki, Japan.

[6] Current address: Division of Regenerative Medicine, Jichi Medical University, Tochigi, Japan.

[7] Current address: Department of Transfusion Medicine, Yokohama City University Hospital, Kanagawa, Japan.

[8] Address correspondence and reprint requests to Dr. Shigeru Chiba, Department of Clinical and Experimental Hematology, University of Tsukuba, 1-1-1 Tennodai, Tsukuba, Ibaraki. E-mail address: schiba-tky@umin.net

[9] Abbreviations used in this paper: CB, cord blood; cy, cytoplasmic; FL, Fms-like kinase 3 ligand; DAPT, *N*-[*N*-(3,5-difluorophenacetyl-L-alanyl)]-*S*-phenylglycine *tert*-butyl ester; CMA, concanamycin A.

www.jimmunol.org/cgi/doi/10.4049/jimmunol.0803036

including various hematopoietic and immune cells (7–9). To date, four Notch receptors (Notch1– Notch4) and at least four Notch ligands (Delta1, Delta4, Jagged1, and Jagged2) have been identified in mammals. Signaling through Notch1 is crucial in the early stages of T cell development (10–12). In culture, ligand-induced Notch signaling drives human CB $CD34^+$ cells to differentiate into T/NK cell precursors (13). Furthermore, Notch signaling drives the T/NK precursors toward differentiation into T and NK cells, although the results for the NK cells are controversial. For example, inhibition of Notch signaling suppresses T cell development and stimulates NK cell development (14–16), whereas activation of Notch signaling contributes to the efficient development of NK cells in mice (17, 18) and humans (19). It is not concluded, however, whether Notch signaling is involved in the function of NK cells or whether IL-15 is necessary for NK cell development in culture.

In this report, to gain further insight into the physiologic significance of Notch signaling in NK cell development, we examined whether IL-15 is dispensable for the generation of functional NK cells and whether Notch signaling has a role in the later stages of NK cell development. Our results indicated that Notch signaling, but not IL-15 stimulation, was essential for inducing $CD34^+$ cells to give rise to $CD7^+$ and cytoplasmic (cy) $CD3^+$ cells that express CD56 in stroma-free culture. Surprisingly, cells cultured with Delta4-coated plates, but lacking IL-15 in the medium, were functional NK cells with cytotoxic activity. IL-15, along with Delta4, further augmented NK cell activity and phenotypic maturation. The addition of IL-15 without exogenous Notch ligand, however, did not allow $CD34^+$ cells to take a NK cell developmental pathway resembling physiologic NK cell precursors. Notch signaling might have a significant role in the development of NK cells in vivo.

Materials and Methods

Reagents and Abs

Recombinant human Delta4-Fc chimeric protein was generated as described previously (20). Recombinant human IL-7 and IL-15 were purchased from R&D Systems. Human stem cell factor and human Fms-like kinase 3 ligand (FL) were a gift from Amgen. Human IL-6/IL-6 receptor fusion protein (FP6) and human thrombopoietin were provided by Kirin Pharma. Anti-IL-15 Ab (MAB2471) and isotype control mouse IgG1 were purchased from R&D Systems. Anti-CD3 (UCHT1), CD8 (SK1), CD14 (M5E2), CD44 (G44-26), CD45 (HI30), CD45RA (HI100), CD56 (B159), CD94 (HP-3D9), CD161 (DX12), NKG2D (1D11), CCR7 (3D12), granzyme B (GB11), and IFN-γ (25723.1) Abs were purchased from BD Biosciences. Anti-CD2 (T11), CD4 (13B8.2), CD7 (8H8.1), CD11a (25.3), CD11b (Bear1), CD25 (B1.49.9), CD27 (1A4CD27), CD33 (D3HL60.251), CD57 (NC1), CD62L (DREG56), CD117 (YB5.B8), CD122 (CF1), CD158a (EB6), and CD158b (GL183) Abs were purchased from Beckman Coulter. Anti-CD34 and CD133 Abs were purchased form Miltenyi Biotec. RIK-2, anti-TRAIL mAb, was prepared as described previously (21).

Isolation of $CD34^+$ and $CD133^+$ cells

Human CB samples were collected from normal full-term deliveries. The parents of all donors provided written informed consent to participate in the study. The procedures were approved by the institutional review board. Mononuclear cells were separated from blood samples by density gradient centrifugation (Lymphoprep; AXIS-SHIELD PoC). CD34- and CD133-enriched cells were separated from mononuclear cells using a MACS Direct CD34 Progenitor Cell Isolation Kit and MACS CD133 MicroBead Kit (Miltenyi Biotec), respectively, according to the manufacturer's protocol. The purity of the $CD34^+$ and $CD133^+$ cells was 97.3 ± 2.3% (n = 15) and 95.4 ± 3.2% (n = 4), respectively. Residual $CD3^+$ and $CD56^+$ cells were 0.73 ± 0.42% and 0.41 ± 0.32%, respectively, in either purification strategy.

Cell culture

Nontissue culture-type 24-well plates were precoated by applying 10 μg/ml Delta4-Fc or control Fc fragments of human Ig G (Fc) (Athens Research & Technology) to the plates at 37°C for 1 h. Cells were cultured in MEM Eagle, α modification (Sigma-Aldrich) supplemented with 20% FBS (Thermo Trace) and penicillin-streptomycin at 37°C in a humidified atmosphere flushed with 5% CO_2 in air. The number of CD34 or CD133 magnetic bead-sorted cells seeded in each well was 0.25–1.2 × 10^5. Cytokines were added at concentrations of 10 ng/ml for IL-7, 100 ng/ml for stem cell factor and 100 ng/ml for FL. one-half of the culture medium was changed every 3 or 4 days. Ten nanograms of thrombopoietin per ml and 100 ng/ml FP6 were added only into the starting culture medium for effective proliferation, although they were not essential (data not shown). IL-15 was added at 5 ng/ml when indicated. Anti-IL-15 or isotype IgG was added at 10 μg/ml when indicated. To inhibit Notch signaling, 10 μmol/L γ-secretase inhibitor *N*-[*N*-(3,5-difluorophenacetyl-L-alanyl)]-*S*-phenylglycine *tert*-butyl ester (DAPT; Calbiochem) was added to the culture medium. $CD161^+$ and $CD161^-$ cells from the culture were isolated using FACSAria (BD Biosciences) after staining with anti-CD161-PE Ab.

Phenotyping assay

Immunofluorescence staining for flow cytometry was performed according to standard procedures. To exclude dead cells from the analysis, 7-aminoactinomycin D (Beckman Coulter) was used. Cytoplasmic staining was performed as follows: after staining the cells with anti-CD56-allophycocyanin and fixing with FACS lysing solution (BD Biosciences), the cells were permeabilized using FACS permeabilizing solution (BD Biosciences) and stained with anti-CD3-PE Ab. For staining for granzyme B, the same fixing and permeabilizing procedure was performed after cell surface staining with anti-CD56-PE and anti-CD3-allophycocyanin. For staining for TRAIL, the cells were incubated with 1 μg of RIK-2 for 30 min at 4°C followed by anti-mouse IgG1-PE (A85-1). Cells were analyzed by flow cytometry using FACSCalibur and CellQuest software (BD Biosciences).

Cytotoxicity assays

A ^{51}Cr release assay to determine cytotoxicity was performed using standard procedures. In brief, 5 × 10^3 K562 or Jurkat cells were labeled with $Na_2{}^{51}CrO_3$ (Amersham Biosciences) and cocultured with effector cells at various ratios in 96-well round-bottom microtiter plates in 200 μl of culture medium. The cocultured cells were incubated for 4 h, and 100 μl of supernatant was collected from each well and counted with a Packard COBRA gamma counter (Packard Instruments). The percentage of specific ^{51}Cr release was calculated as follows: [cpm experimental release − cpm spontaneous release]/(cpm maximal release − cpm spontaneous release) × 100. The ratio of spontaneous release to maximal release was <20% in all experiments. In experiments to test the mode of cytotoxicity, we used concanamycin A (CMA; Sigma-Aldrich) as a selective inhibitor of the perforin-mediated cytotoxicity, and anti-TRAIL Ab RIK-2. Effectors were pretreated with 100 nmol/L CMA for 2 h before the cytotoxicity assays (22). RIK-2 was added at a final concentration of 10 μg/ml at the start of the cytotoxicity assay.

Intracellular cytokines

The cells were stimulated by PMA (25 ng/ml; Sigma-Aldrich) and ionomycin (1 μg/ml; Sigma-Aldrich) in the presence of monensin (2 μmol/L; Sigma-Aldrich) for 4 h. After staining the cells with anti-CD56-PE, they were fixed and permeabilized as described above and stained with anti-IFN-γ-FITC Ab. The cells were analyzed on a FACSCalibur using CellQuest software.

Anti-Notch Abs

For cell surface staining, we used biotinylated Abs and streptavidin-PE (BD Biosciences). To block Notch1, we added 10 (μg/ml) MHN1-519 to the medium. Mouse IgG1 (R&D Systems) was used as the control. The anti-human Notch1 (MHN1-519, mouse IgG1), Notch2 (MHN2-25, mouse IgG2a), and Notch3 (MHN3–21, mouse IgG1) mAbs were generated by immunizing BALB/c mice with human Notch1-Fc (R&D Systems), Notch2-Fc (the Fc portion of human IgG1 was fused to the 22nd epidermal growth factor repeat of the extracellular region of human Notch2), or Notch3-Fc (R&D Systems) and screening hybridomas producing mAbs specific for Notch1-Fc, Notch2-Fc, or Notch3-Fc by ELISA. MHN1-519, MHN2-25, and MHN3-21 reacted with CHO(r) cells (23) expressing human Notch1, Notch2, and Notch3, respectively, as demonstrated by flow cytometry (supplemental Fig. S4*A*[10]). MHN1-519 and MHN3h21 blocked Notch1-Fc and Notch3-Fc binding to CHO(r) cells expressing human Delta4, respectively, but MHN2-25 did not block Notch2-Fc binding (supplemental Fig. S4*B*).

[10] The online version of this article contains supplemental material.

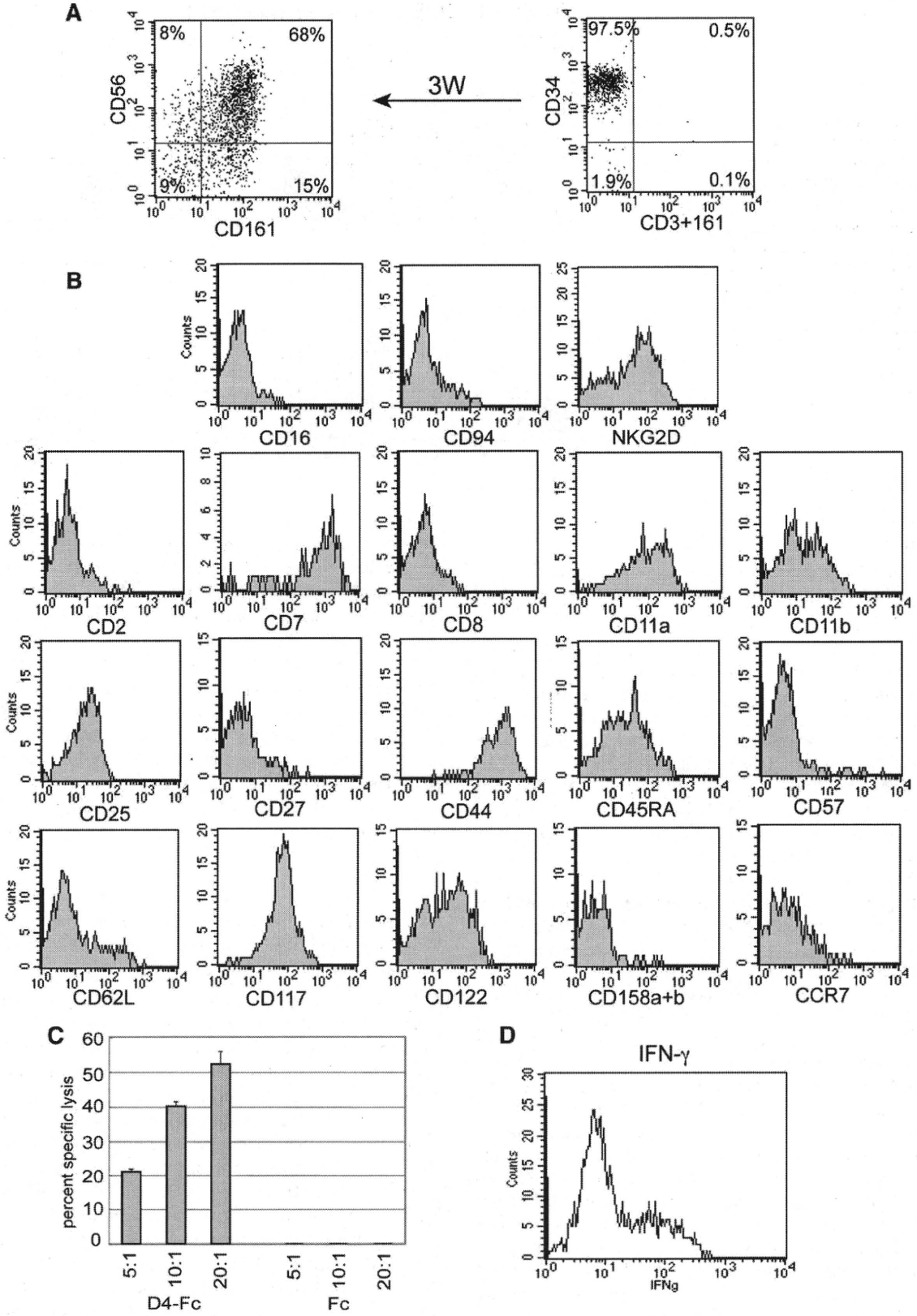

FIGURE 1. Phenotypic and functional analysis of cells derived from $CD34^+$ cells on Delta4-Fc-coated plates. *A*, Representative dot plot illustrating CD161 vs CD56 expression in the cells generated on Delta4-Fc-coated plates from $CD34^+$ CB cells after culture for 3 wk, and dot plot illustrating CD161/CD3 vs CD34 of the sorted CB population before culture. *B*, Various phenotypic analyses of the 3-wk cultured cells that were gated on $CD161^+$ events. Results are representative of at least four experiments. *C*, The 2.5-wk cultured cells were cytotoxic against K562 target cells at the indicated E:T ratios. The ratio of $CD161^+$ cells cultured on Delta4-Fc-coated plates and those Fc-coated plates in this experiment was 40 and 0%, respectively. Results are representative of four experiments. *D*, IFN-γ production by the 3-wk culture cells, as analyzed by intracellular expression. The histogram plots were gated on $CD56^+$events. Results are representative of five experiments.

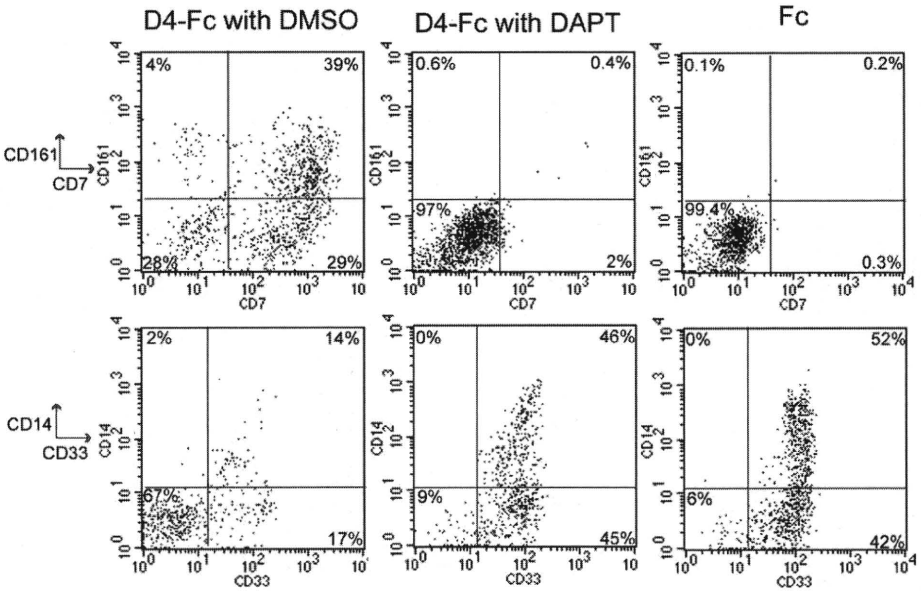

FIGURE 2. Phenotypic analysis of cells cultured in the presence of γ-secretase inhibitors. Representative dot plots of CB CD34$^+$ cells that were cultured for 2.5 wk on Delta4-Fc-coated plates with DMSO (the solvent for the γ-secretase inhibitors: D4-Fc with DMSO), Delta4-Fc-coated plates with DAPT (D4-Fc with DAPT), and Fc-coated plates (Fc). Results are representative of three experiments.

Results

Human CB CD34$^+$ and CD133$^+$ cells gave rise to functional NK cells by Notch signaling in a stroma-free culture without exogenous IL-15

CD34$^+$ or CD133$^+$ cells were cultured on Delta4-Fc-coated plates. The cells became almost immunophenotypically homogeneous after culture for ~3 wk (Fig. 1*A*). The proliferation efficiency depended on CB batches; fold increases in the cell number after the 3-wk culture were 10.3 ± 7.74-fold (n = 11). These cells expressed CD56 and CD161, but did not express surface CD3 or TCRα/β (data not shown). CD56/CD161 double-positive cells also expressed NKG2D and CD117, but were essentially negative for CD16 and killer Ig-like receptors (CD158a and CD158b). The cells had cytotoxic activity against K562 (Fig. 1*C*) and Jurkat cells (see Fig. 5*Bii*), and secreted IFN-γ (Fig. 1*D*). These results indicate that the culture products meet the general criteria for functional NK cells. The products generated from CB CD34$^+$ and CD133$^+$ had the same characteristics (data not shown).

Virtually no NK cells developed in culture on control Fc-coated plates; the vast majority of the cells were CD33$^+$ myeloid cells, a significant part of which expressed CD14 (Fig. 2). The absolute cell numbers with control Fc are ~5-fold higher than that with Delta4-Fc, and the fold increases in the cell number after the 3-wk culture were 45.7 ± 31.6-fold (n = 11). To confirm that the NK cell differentiation was Notch dependent, we added a γ-secretase inhibitor, DAPT, which strongly inhibits ligand-dependent Notch activation (24, 25). The cells cultured on Delta4-Fc-coated plates in the presence of DAPT had the same immunophenotype as those cultured on the control Fc-coated plates and did not give rise to NK cells (Fig. 2), indicating that the observed NK cell development was Notch activation dependent. The number of cells generated increased to the level of that in the control Fc protein-coated plates (data not shown).

We cultured CD34$^+$ cells and CD133$^+$ cells purified from G-CSF-mobilized peripheral blood cells. Both cell types gave rise to CD56$^+$CD161$^+$ NK cells that were similar to those derived from CB CD34$^+$ or CD133$^+$ cells. The amount of time required for mobilized peripheral blood CD34$^+$ or CD133$^+$ cells (~5 wk) to develop to a major population of CD56$^+$CD161$^+$ NK cells was greater than that required for CB CD34$^+$ or CD133$^+$ cells (supplemental Figs. S1*A* and S2 and Fig. 3), although the time courses varied to some degree from batch to batch (supplemental Fig. S2 and data not shown).

We next examined the effects of other soluble Notch ligands, human Delta1-Fc and Jagged1-Fc, on NK cell development from CB CD34$^+$ cells. Delta1-Fc had an effect similar to that of Delta4-Fc, although with lower efficiency (supplemental Fig. S1*B*), and Jagged1-Fc showed no potential to induce NK cell development (data not shown). Therefore, we used Delta4-Fc as the soluble Notch ligand and CB CD34$^+$ cells as the starting material for the remaining experiments.

IL-15 is dispensable for in vitro NK cell development from CB CD34$^+$ cells in the presence of Delta4 stimulation, whereas Notch stimulation appears to be essential for physiologic NK cell development

When IL-15 was added to the culture medium on control Fc-coated plates, CD56$^+$CD161$^+$ NK cells emerged (Fig. 3 and supplemental Fig.S2, Fc plus IL-15; cf with Fig. 3 and supplemental Fig.S2, Fc); this effect was blocked by anti-IL-15- neutralizing Ab (Fig. 3 and supplemental Fig.S2, Fc plus IL-15 plus anti-IL-15). IL-15 does not affect the absolute cell number; fold increases in the cell number after the 3-wk culture were 46.8 ± 36.3-fold, 43.1 ± 35.7-fold, and 48.4 ± 9.48-fold with IL-15 (n = 7), without IL-15 (n = 7), and with IL-15 and anti-IL-15 (n = 3) in the control Fc-coated plate condition. The rate of NK cell development by IL-15 stimulation, however, was much slower than that by Delta4-Fc stimulation. In the absence of Notch stimulation, but with IL-15, the percentage of total NK-lineage cells represented by positive CD161 was only 2.6 ± 2.9%, 6.3 ± 4.6%, and 9.0 ± 4.5% at 2, 3, and 4 wk, respectively (Fig. 3 and supplemental Fig.S2, Fc plus IL-15); whereas in Delta4-Fc with IL-15 (Fig. 3 and supplemental Fig.S2, D4-Fc plus IL-15) or without IL-15 (Fig. 3 and supplemental Fig.S2, D4-Fc), the percentage of total NK-lineage cells was 56 ± 17%, 77 ± 11%, and 81 ± 5.8% (with IL-15) or 52 ± 18%, 74 ±

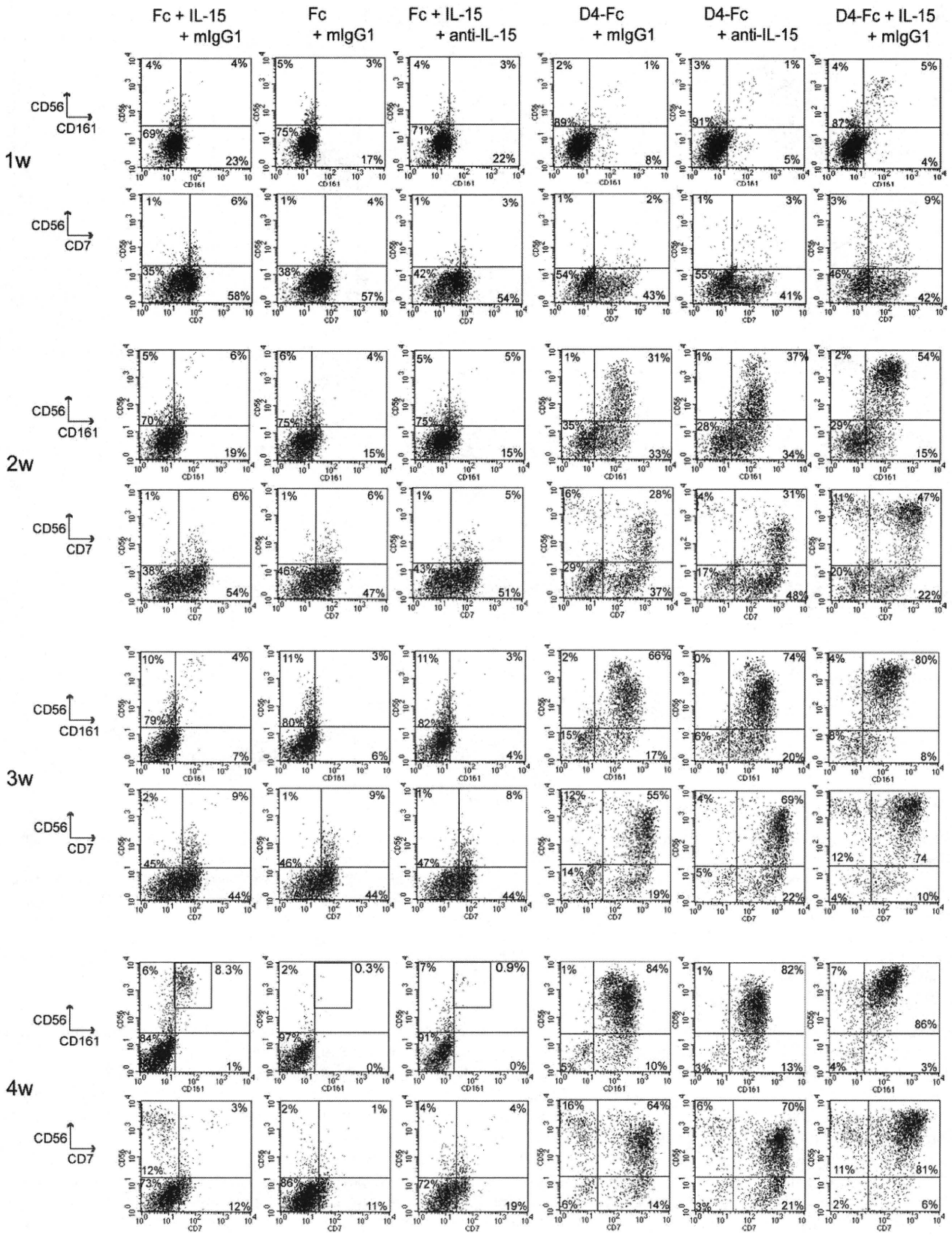

FIGURE 3. Phenotypic analysis during culture under several culture conditions. Representative dot plots illustrating CD161 vs CD56 and CD7 vs CD56 of cells that were cultured from CB CD34$^+$ cells for the indicated number of weeks on Fc-coated plates with IL-15 and mouse (m) IgG1-containing medium (Fc + IL-15 + mIgG1), Fc-coated plates with mouse IgG1-containing medium (Fc + mIgG1), Fc-coated plates with anti-IL-15 Ab-containing medium (Fc + anti-IL-15), Delta4-Fc-coated plates with mouse IgG1-containing medium (D4-Fc + mIgG1), Delta4-Fc-coated plates with anti-IL-15 Ab-containing medium (D4-Fc + anti-IL-15), and Delta4-Fc-coated plates with IL-15 and mouse IgG1-containing medium (D4-Fc + IL-15 + mIgG1). Results are representative of at least three experiments. The means and SD of each CD161 vs CD56 quadrant in replicate experiments are shown in supplemental Fig. S2.

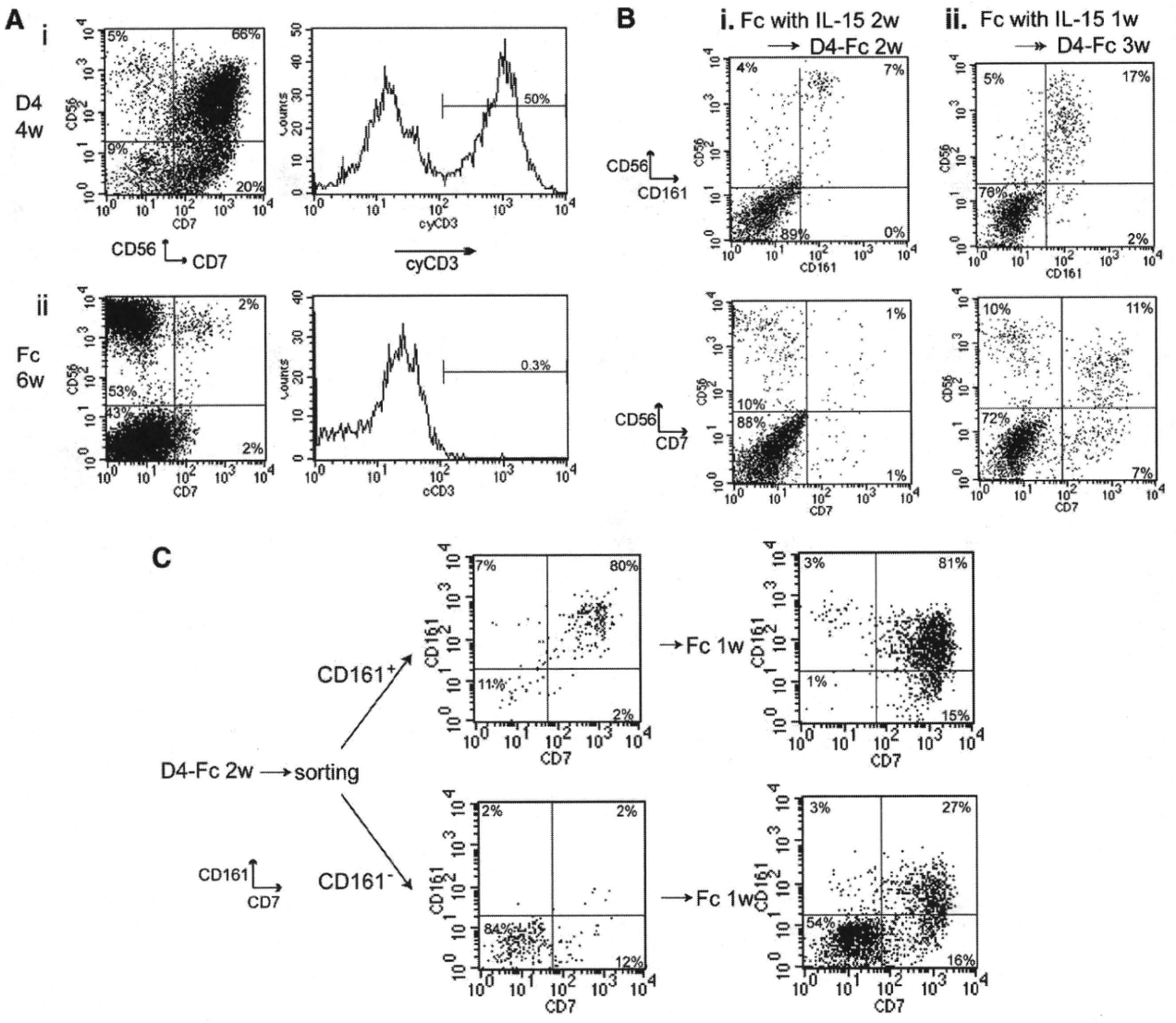

FIGURE 4. Phenotypic analysis of cells after various culture conditions. *A*, Representative dot plots illustrating CD7 vs CD56 cells that were cultured from CB $CD34^+$ cells for 4 wk on Delta4-Fc-coated plates (D4, *Ai*) and for 6 wk on Fc-coated plates in the presence of IL-15 (Fc, *Aii*). Histogram plots illustrating cyCD3 of the same cells that were gated on $CD56^+$ events. Results are representative of six and five experiments, respectively. *B*, Representative dot plots of cells that were cultured from CB $CD34^+$ cells for 2 or 1 wk on Fc-coated plates with IL-15-containing medium and were then transferred to Delta4-Fc-coated plates and cultured for 2 or 3 wk, respectively, with IL-15-free medium (*Bi* and *Bii*). Results are representative of three experiments. *C*, Representative dot plots illustrating CD7 vs CD161 expression in the cells that were sorted into $CD161^+$ or $CD161^-$ after 2-wk culture from CB $CD34^+$ cells on Delta4-Fc-coated plates, and dot plots of cells that were cultured another week on Fc-coated plates with IL-15-free medium. Results are representative of three experiments.

11%, and 88 ± 6.7% (without IL-15) at 2, 3, and 4 wk, respectively. (supplemental Fig. S2*Bi*) The differences were statistically significant between the D4-Fc group and the Fc group ($p < 0.001$). The adjusted absolute numbers of NK-lineage cells cultured on Delta4-Fc tended to be greater than those cultured on Fc with IL-15, although the differences were not always statistically significant (supplemental Fig. S3*C*). $CD56^+$ $CD161^+$ NK cells eventually comprised a major population after 6 wk of culture with IL-15 but without Notch stimulation (Fig. 4*Ai*). No $CD56^+CD7^+$ (Fig. 3, Fc plus IL-15) or $CD56^+$ $cyCD3^+$ (Fig. 4*Aii*) cells were detected during culture with IL-15 but without Delta4-Fc, whereas Delta4-Fc stimulation induced the generation of $CD7^+cyCD3^+$ cells, which could represent naturally arising T/NK cell progenitors (26, 27), at the early phase of the culture. Although $CD7^{low}$ cells appeared in culture with IL-15 alone, they might represent monocytes, because a substantial amount of $CD14^+$ cells emerged regardless of the presence of IL-15 when Delta4-Fc was absent and peripheral blood monocytes express CD7 at low levels.

Delta4-Fc stimulation without IL-15 efficiently induced NK cell development (Figs. 1 and 3 and supplemental Fig. S2, D4-Fc). Most of the cells became $CD7^{high}$ in the first 2 wk. A few $CD161^+$ cells were detected at the first week, the number of which increased at the next week. Only a part of the $CD161^+$ cells was positive for CD56 during the early phase of the culture, but at the later time points, most $CD161^+$ cells were $CD56^+$. This observation may indicate that $CD161^+CD56^-$ cells emerge at first and they gradually become $CD161^+$ $CD56^+$, although there is another interpretation such as simultaneous generation of double-positive and CD161 single-positive cells, expansion of double-positive cells, and apoptotic disappearance of the single-positive cells. Given the previous

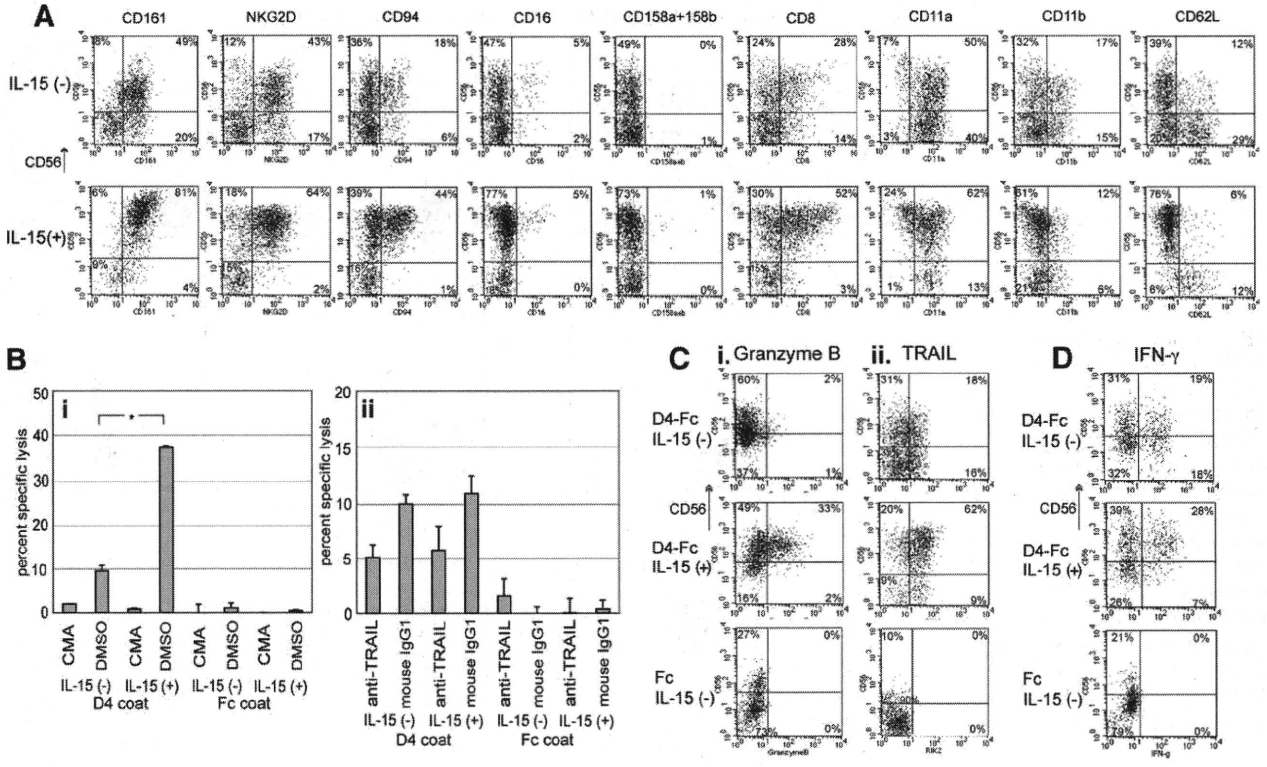

FIGURE 5. Phenotypic and functional differences between cells cultured in IL-15-containing and IL-15-free medium on Delta4-Fc-coated plates. *A*, Representative dot plots illustrating CD56 vs indicated Ags of cells cultured for 3 wk from CB CD34$^+$ cells in IL-15-containing or IL-15-free medium on Delta4-Fc-coated plates. Results are representative of six experiments. *B*, Cytotoxicity against K562 (*Bi*) or Jurkat (*Bii*) target cells at an E:T ratio of 5:1. Effectors were developed in the indicated conditions for 2.5 wk. In this experiment, the ratio of CD161$^+$ cells cultured on Delta4-Fc-coated plates with or without IL-15 condition and those cultured on Fc-coated plates with or without IL-15 condition were 53, 46, 0.6, and 0%, respectively. Effectors were pretreated with CMA or DMSO (the solvent for CMA) (*Bi*). Anti-TRAIL RIK-2 or its isotype control mouse IgG1 was added at the start of the cytotoxicity assay (*Bii*). Results are representative of three (*Bi*) and six (*Bii*) experiments. Batch to batch variation can be seen by comparing this figure with Fig. 1. *C*, Representative dot plots illustrating intracellular granzyme B (*Ci*) or TRAIL (*Cii*) vs CD56 of the cells cultured for 3 wk in medium with or without IL-15 on Delta4-Fc-coated plates and without IL-15 on Fc-coated plates. Results are representative of four experiments. *D*, Representative dot plots illustrating intracellular IFN-γ vs CD56 of cells cultured for 3 wk in medium with or without IL-15 on Delta4-Fc-coated plates and without IL-15 on Fc-coated plates. Results are representative of four experiments.

demonstration that CD161 is expressed on the cell surface earlier than CD56 (28), the former possibility appears more likely. To explore the possibility that IL-15 is secreted by a certain population of cells during culture and contributes to NK cell development, we added anti-IL-15-neutralizing Ab to the culture. The addition of anti-IL-15-neutralizing Ab to the culture medium blocked NK cell development in the presence of IL-15 (Fig. 3, IL-15 plus anti-IL-15), but did not affect either the rate or efficiency of Delta4-Fc-dependent NK cell emergence (Fig. 3, D4-Fc plus anti-IL-15, fold increase in the cell number after 3-wk culture on Delta4-coated plate with anti-IL-15 was 8.75 ± 4.18-fold (n = 5), which was not statistically different from those cultured on Delta4-coated plates without anti-IL-15 or with IL-15), further supporting the possibility that IL-15 is dispensable for NK cell development from human CB CD34$^+$ cells.

IL-2 is also suggested to be involved in the NK cell development. To examine whether IL-2, which might be secreted by a certain population of the cells, was present in the culture, the IL-2 concentration in the supernatant was measured by ELISA. No IL-2 was detected (cutoff level, 7 pg/ml; data not shown), indicating that IL-2 was not involved in the NK cell development induced by Delta4-Fc.

To examine the NK cell developmental stages that are critically dependent on Notch signaling, we cultured CB CD34$^+$ cells on control Fc-coated plates with IL-15 for 1 or 2 wk and then transferred them onto Delta4-Fc-coated plates and cultured them further for 3 or 2 wk without IL-15, respectively (culturing for a total of 4 wk). Approximately 50% of the CD56$^+$ CD161$^+$ population expressed CD7$^+$ at 4 wk in the 1-wk IL-15 condition (Fig. 4*Bii*). In contrast, very few CD56$^+$ cells that emerged in the 2-wk IL-15 condition expressed CD7 (Fig. 4*Bi*). These observations indicated that CB CD34$^+$ cells cultured with IL-15, but without Notch stimulation, for 1 wk retained the capacity to generate CD56$^+$CD7$^+$ cells, but that they lost this capacity when cultured without Notch stimulation for 2 wk. We also examined whether the Notch stimulation at early phases of the culture irreversibly determines NK cell developmental fate. To examine the early phase of NK cell development, we cultured CB CD34$^+$ cells for 2 wk on Delta4-Fc-coated plates and sorted the product into CD161$^+$ and CD161$^-$ cells, because CD161 is known to be expressed earlier than CD56 on the cell surface (28). We then transferred each population onto control Fc-coated plates and cultured them for another week without IL-15. More than 80% of the population derived from the CD161$^+$ cells expressed CD7$^+$. Interestingly, the CD161$^-$ cells also gave rise to CD161$^+$CD7$^+$ cells among one of the two major populations (Fig. 4*C*). These observations indicate that Notch activation irreversibly drives a subset of CD34$^+$ cell

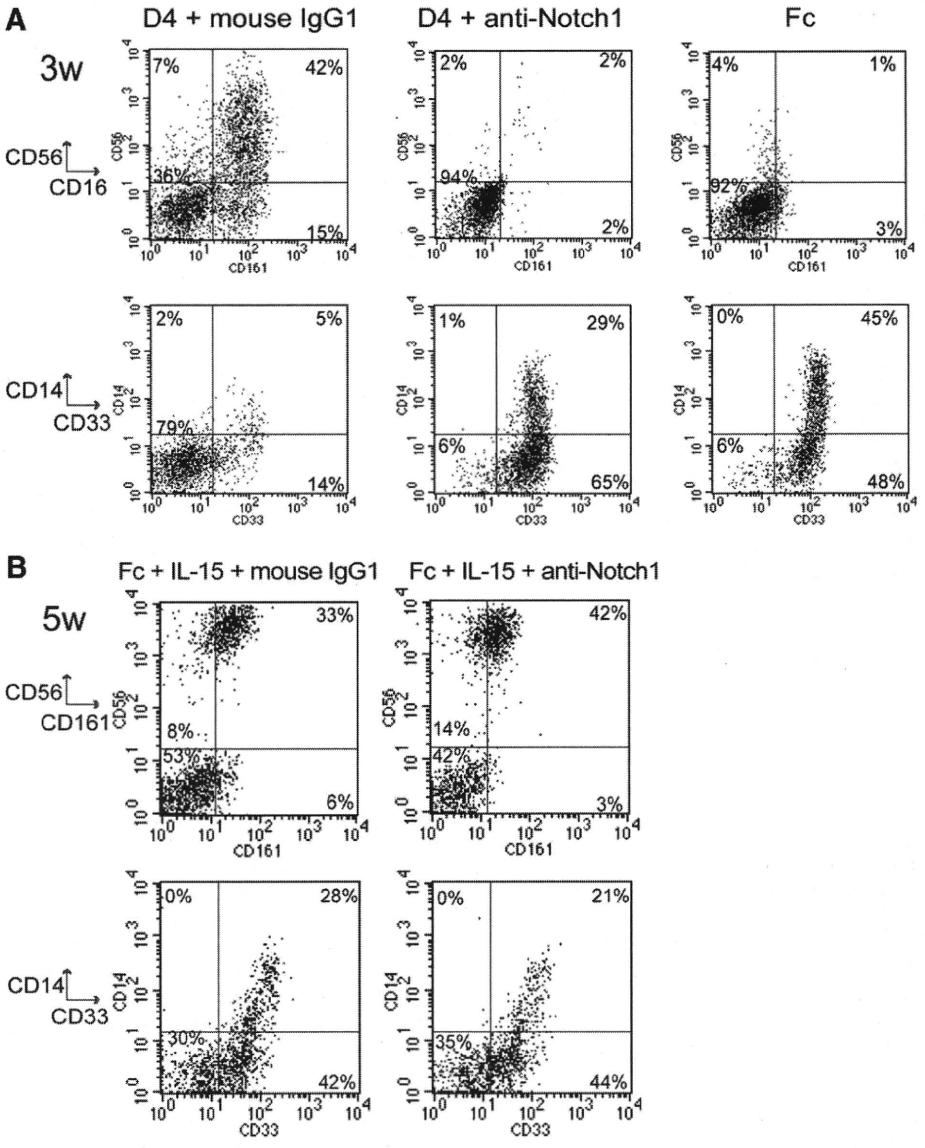

FIGURE 6. Phenotypic analysis of cells cultured in the presence of human Notch1-blocking Ab. *A*, Representative dot plots of cells that were cultured for 3 wk from CB $CD34^+$ cells on Delta4-Fc-coated plates with mouse IgG1-containing medium, Delta4-Fc-coated plates with anti-human Notch1-containing medium, and Fc-coated plates. Results are representative of six experiments. *B*, Representative dot plots of cells that were cultured for 5 wk from CB $CD34^+$ cells on Fc-coated plates with IL-15 and mouse IgG1-containing medium and Fc-coated plates with IL-15 and anti-human Notch1-containing medium. Results are representative of three experiments.

progenies to the $CD161^+CD7^+$ NK cell fate within 2 wk, presumably before $CD161^+$ is expressed.

IL-15, along with Delta4 stimulation, induces phenotypic maturation and functional augmentation of CB $CD34^+$ cell-derived NK cells

We compared the immunophenotype of the CB $CD34^+$ cell-derived NK cells generated in the culture with Delta4-Fc but lacking IL-15 (D4-Fc) and in culture with Delta4-Fc and IL-15 (D4-Fc plus IL-15). IL-15 does not affect the absolute cell number; fold increases in the cell number after the 3-wk culture were 10.6 ± 6.16-fold and 10.2 ± 6.71-fold with and without IL-15 in the D4-Fc-coated plate condition (n = 8). The cells grew slightly faster with D4-Fc plus IL-15 than with D4-Fc alone, but there were no significant differences in the frequency of $CD56^+CD161^+$ population in both conditions after 3 wk (cf Fig. 3 and supplemental Fig. S2*A*, D4-Fc and D4-Fc plus IL-15; supplemental Fig. S2*Bii*; and Fig. 5). The expression levels of CD7 and NKG2D were similar. CD94 was expressed at a higher level in the D4-Fc plus IL-15 condition. CD16 and CD158 were not expressed in the D4-Fc condition, but were expressed at low levels in the D4-Fc plus IL-15 condition. The expression levels of adhesion molecules, i.e., CD11a, CD11b, and CD62L, were higher in the D4-Fc condition (Fig. 5*A*). The other markers shown in Fig. 1 (CD2, CD7, CD25, CD27, CD44, CD45RA, CD57, CD117, CD122, and CCR7; data not shown), as well as IFN-γ (Fig. 5*D*), were expressed at similar levels under both conditions. There was a remarkable difference in the expression level of CD56, which was markedly higher in the D4-Fc plus IL-15 condition.

Cytotoxic activity against K562 cells was significantly higher in NK cells generated in the D4-Fc plus IL-15 condition than that in the D4-Fc condition. CMA, an inhibitor of perforin-mediated cytotoxicity, had a stronger suppressive effect on the cytotoxic activities of NK cells generated in the D4-Fc plus IL-15 condition (Fig. 5*Bi*). Interestingly, granzyme B, which enhances the perforin-mediated cytotoxicity and whose expression was not detected in the D4-Fc condition, was up-regulated in the D4-Fc plus IL-15 condition (Fig. 5*Ci*). This might explain the stronger suppression of NK cell cytotoxic activity by CMA when generated in the D4-Fc plus IL-15 condition compared with the D4-Fc condition. In contrast, there was no significant difference in the killing activities against Jurkat cells of the NK cells generated under